CHALMERS

Control and Disturbance Rejection

of a ground stabilization process

Johan Larsson

Department of Signals and Systems
CHALMERS UNIVERSITY OF TECHNOLOGY
Göteborg, Sweden

EX038/2014

Abstract

As preparation for building of roads and railroads on damp ground, the ground
sometimes needs to be stabilized. This can be done by ejecting limestone into the
ground. A way to do this is by drilling into the ground and eject a mixture of
cement and limestone thus creating a pillar. AcobiaFLUX has developed a system
for supervising and controlling a procedure like this. They measure the depth of the
drilling tool and the weight of the material stored in a tank and plot the depth on
the vertical axis and average ejected mass per meter on the horizontal axis of a graph
visible for the operator. Disturbances causes the graph to get out of hand sometimes
and there are substantial fluctuations. This means that the client performing the
ground stabilization cannot rely on what is visible in the graph. Attempts have
been made, with varying results, to suppress these disturbances by averaging the
process output. The underlying reasons for the thesis is the need of a better way of
disturbance rejection as well as an improved automatic controller for the process.
In the thesis, different ways of estimating the ejected mass per meter, filtering the
quantity and automatically control it has been investigated. In order to better
understand the process and to evaluate different filter and control configurations,
a mathematical model was derived using mass balance, differential flow equations
etc. Simulations showed that a moving average estimation of the quantity using
the tank mass and the depth of the tool together with a first order low pass filter
was a suitable way of estimating the ejected mass per meter. A PID_f controller
with anti-windup filter proved to be able to keep the estimated ejected mass per
meter within the tolerance levels during steady state. The filter and the controller
was implemented in a SCADA environment and simulated once more and also here
proven to be suitable for the task. Experiments on a real machine showed improved
results compared to the old controller configuration although some tuning might be
needed.

KEYWORDS: modeling, control, process, disturbance, filtering

Sammanfattning

Som förberedelse för byggandet av vägar och järnvägar på fuktig mark behöver marken ibland stabiliseras. Detta kan göras genom att spruta in kalksten i marken. Ett sätt att göra detta är att borra sig ner i marken och mata ut en blandning av cement och kalk och på så sätt skapa en pelare. AcobiaFLUX har utvecklat ett system för att övervaka och styra en sådan process. De mäter djupet på borrverktyget och vikten av materialet i en tank och plottar djupet på den vertikala axeln och genomsnittlig utsprutad massa per meter på den horisontella axeln i en graf synlig för operatören. Störningar orsakar stora variationer i processen vilket innebär att kunden som utför markstabiliseringen inte kan lita på vad som syns i grafen. Försök har gjorts, med varierande resultat, att dämpa dessa störningar genom att göra glidande medelvärdesberäkningar på utsignalen. De bakomliggande orsakerna till detta examensarbete är behovet av ett bättre sätt att filtrera bort störningarna samt en förbättrad automatisk styrning av processen. Olika sätt att uppskatta kvantiteten *utsprutad massa per meter*, filtrering av den och automatiskt reglering av den har undersökts. För att bättre förstå processen och för att kunna utvärdera olika filter och typer av reglering, konstruerades en matematisk modell med hjälp av massbalans och differentialekvationer. Simuleringar visade att den utsprutade massan per meter kunde skattas med hjälp utav en glidande medelvärdesskattning. Denna skattning tillsammans med ett första ordningens lågpassfilter visade sig vara lämpligt. En PID_f-regulator med anti-windup-filter visade sig kunna hålla den skattade utsprutade massan per meter inom toleransnivåerna i steady state. Filtret och regulatorn implementerades sedan i en SCADA-miljö och simuleringar i denna miljö visade också tillfredställande resultat. Experiment på en riktig maskin visade ett förbättrat resultat jämfört med den gamla reglerkonfigurationen även om viss tuning kan behövas.

NYCKELORD: reglering, process, filter, störningar, modellering

Preface

The thesis has been done at a company called AcobiaFLUX for a client, Dmixab. AcobiaFLUX is a company oriented in automation and industrial IT. They develop systems for control and monitoring of processes in industry, infrastructure and real estate.

Acknowledgments

I would like to thank Nibben Peterzéns at Dmixab for helping with describing the ground stabilization process and answering questions, my supervisor at AcobiaFLUX, Henrik Johansson, for helping me throughout the work and helping with the implementation. Last but not least i would like to thank Bo Egardt who has been my supervisor at Chalmers and helped me with theoretical parts of the thesis as well as report writing. Also, thanks to everyone at AcobiaFLUX who made it possible to write my thesis in an industrial environment.

Göteborg, June 16, 2014

JOHAN LARSSON

CONTENTS

x

1 Introduction

This section gives an introduction to the thesis. A background to the use of controllers in industry as well as ground stabilization is given, followed by the purpose and objectives of the thesis. Necessary delimitations for the thesis are also presented here. The introduction ends with the report outline.

1.1 Background

Ever since the beginning of the twentieth century, automatic controllers have been used in industrial processes. Although back then, the use was very sporadic and automatic control of processes did not become widespread until the mid 1920's. At that time instruments and the theoretical knowledge was not sufficient in order for effective implementation of controllers (Bennett 1993). Also mentioned by (Bennett 1993) is that automatic controllers were often of on-off type which means that the control action was either on or off. This controller consisted of relays controlled by either a solenoid, a motor or pneumatics. A substantial problem with these controllers were the wear on the plant they were implemented on. Later, wide band proportional controllers were developed followed by the adding of derivative and integral action. Nowadays, a majority of industrial processes are automatically controlled and a large number of studies have been made on the subject developing a variety of control strategies.

This thesis project concerns monitoring and control of a specific industrial process. As preparation for building of roads and railroads on damp ground, the ground sometimes needs to be stabilized. This can be done by ejecting limestone into the ground. AcobiaFLUX has a client who drills their way into damp ground and ejects a mixture of cement and limestone, thus creating a pillar. AcobiaFLUX has developed a system for supervising the procedure. They measure the depth of the hose outlet and the weight of the material stored in a tank and plot the depth on the vertical axis and average mass ejected per meter on the horizontal axis of a graph visible for the operator. Disturbances causes the graph to get out of hand sometimes and there are substantial fluctuations. This means that the client cannot rely on the calculations performed in the system and what is visible in the graph. Attempts have been made, with varying results, to suppress these disturbances by averaging the measured signals. The underlying reasons for the thesis is the need of a better way of disturbance rejection as well as an improved automatic controller for the process.

1.2   Purpose and objectives

The purpose of this thesis is to gain knowledge regarding how filters and controllers can be used to stabilize a ground stabilization process subjected to disturbances. Investigated controllers are PID and PID_f with saturation on the control signal and anti-windup filter. Investigated filters are linear phase FIR-filters designed using the Parks-McClellan algorithm, differentiator filter and first order low pass filters. The objectives of the thesis are

- to mathematically model the ground stabilization process

- to compare ways of estimating the quantity *ejected mass per meter*

- to design a filter for disturbance rejection

- to design a controller for automatic ground stabilization with the following controller goals:

  - The controller should make the process output follow a reference value.
  - The controller should keep the process output between the tolerance levels at all times during steady state. The tolerance levels are defined as $\pm 10\%$ of the reference value.
  - The controller should keep the magnitude of the total error below 0.5 kg/m in steady state.

- to simulate and compare filters and controller configurations together with the mathematical model

- to implement a filter and a controller in Cicode(programming language used in CitectSCADA) and simulate it in a SCADA environment

1.3   Delimitations

A couple of delimitations have been made in order to make the problem manageable. The following delimitations have been made:

- In the mathematical model, a number of approximations and assumptions are made in order to keep the complexity of the problem down. These are further explained in Chapter 4.

- For the control design, research is narrowed down to PID and PID_f-control. This is due to nonlinearities in the process which makes for example LQR and linear MPC-control difficult to design. Another reason is that the implementation demands that the number of calculations performed between samples are limited.

1.4 Report outline

The report consists of the following chapters.

Chapter 2 explains capital letters, small letters and greek letters used in modeling as well as abbreviations used in the report.

Chapter 3 describes the ground stabilization process. Inputs and outputs are presented as well as a description of the user interface seen by the operator and current methods of disturbance rejection and control used in the process.

Chapter 4 presents a mathematical model of the process. Mass balance equations together with differential flow and position equations are derived forming a state space model. Controllability and observability are also analyzed here.

Chapter 5 discusses different filter design methods and estimation methods. This includes relevant theory, design methods and simulations.

Chapter 6 discusses ways of automatically controlling the process. This includes relevant theory, design methods and simulations.

Chapter 7 presents the results of the implementation. This includes an explanation of the implemented algorithms as well as simulation results in SCADA.

Chapter 8 discusses the results, what goals are fulfilled and what could be improved. Here is also a conclusion of the thesis presented.

2 Notation

Abbreviations

FFT	fast fourier transform
FIR	finite impulse response
IIR	infinite impulse response
LQR	linear-quadratic regulator
MA	moving average
MPC	model predictive control
PID	proportional integral derivative
PID_f	proportional integral derivative filter
PLC	programmable logic controller
SCADA	supervisory control and data acquisition
SQL	structural query language

Capital Letters

A_h	hose cross sectional area (m^2)
A_t	tank cross sectional area (m^2)
K_{aw}	anti-windup gain
K_d	derative gain of PID-controller
K_i	integral gain of PID-controller
M_t	starting mass in tank (kg)
K_p	proportional gain of PID-controller
Q_h	flow in hose (m^3/s)
$Q_{h,0}$	flow in hose due to height difference between bottom of tank and bottom of drilled hole (m^3/s)
$\hat{Q}_h$	estimated flow in hose (m^3/s)
T_s	sampling time (s)
X	ejected mass per meter (kg/m)
X_f	filtered ejected mass per meter (kg/m)
$\hat{X}$	estimated ejected mass per meter (kg/m)
$\hat{X}_f$	filtered estimated ejected mass per meter (kg/m)

Small Letters

|	
d	disturbance signal (kg)
g	gravitational constant (m/s^2)
h_o	hose outlet position (m)
$h_{o,tot}$	total drilled length (m)
h_v	vehicle height (m)
l_h	length of hose (m)
l_m	moving average span in SCADA (m)
m_t	mass in tank (kg)
m_h	mass in hose (kg)
p_h	pressure difference in hose (N/m^2)
t	time (s)
t_m	time span for moving average (s)
v	rise speed of tool (m/s)
v_h	material speed in hose (m/s)

Greek Letters

ϕ	hose angle (rad)
ρ	mass density (kg/m^3)
α	first order low pass filter constant

3 The Process

This chapter aims to describe the process which the thesis revolves around. First the different parts of the ground stabilization machine are described as well as the procedure of stabilizing the ground. This is followed by a definition of the inputs and outputs of the process as well as a presentation of current methods used for disturbance rejection and control of the process.

3.1 Equipment

The machine performing the ground stabilization consists of a few parts. There is a tank in which a mixture of cement and limestone is stored. This tank is pressurized with an air compressor. Next to the tank, there is a compartment for the operator. Attached to the tank is a hose and the material flow between the tank and hose is controlled with a valve which is either open or closed. To prevent the hose from clogging, air is injected into the hose. The hose is about 50 meters long in total and approximately the 20 last meters of the hose is contained within a drilling tower. At the end of the hose is a tool that could most easily be described as a whisk. The rotational and vertical speed of the tool are controlled by two hydraulic motors.
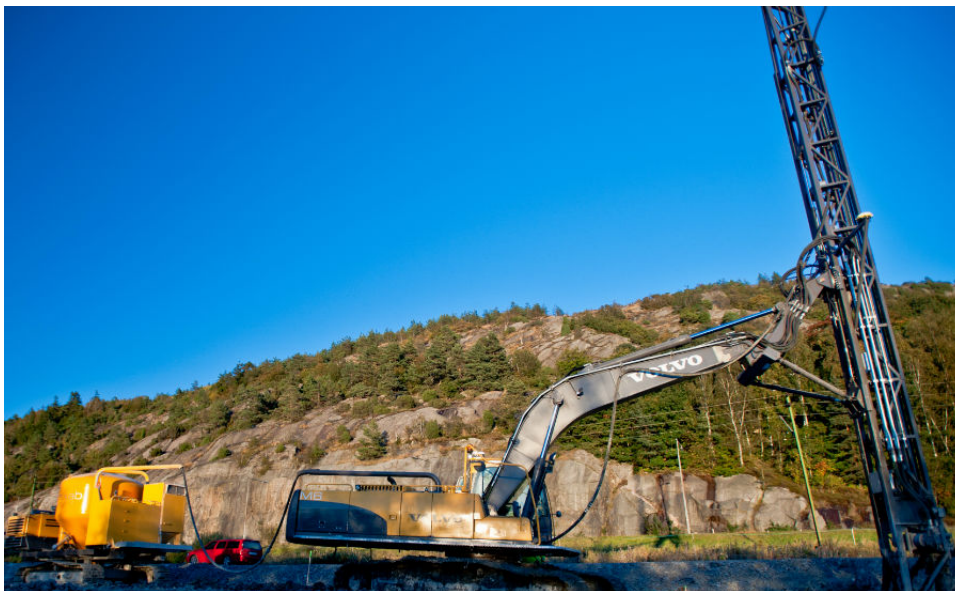

Figure 3.1: *Picture of a machine performing ground stabilization.*

In Figure 3.1 (Dmixab 2014-03-12), a ground stabilization machine is displayed. The tank, operator compartment, hose and drilling tower are visible in the figure.

3.2 Ground Stabilization

The process consists of a tool that drills its way into the ground. When a preset depth is reached, a portion of the mixture is ejected in order to fill the space between the end of the tool and the hose outlet. After this space is filled, the tool starts moving upwards while ejecting material. When the tool reaches a certain depth, the valve closes and the material that is left in the hose is ejected. When this procedure is completed, a pillar has been created. GPS is used to determine the positions to place the pillars.
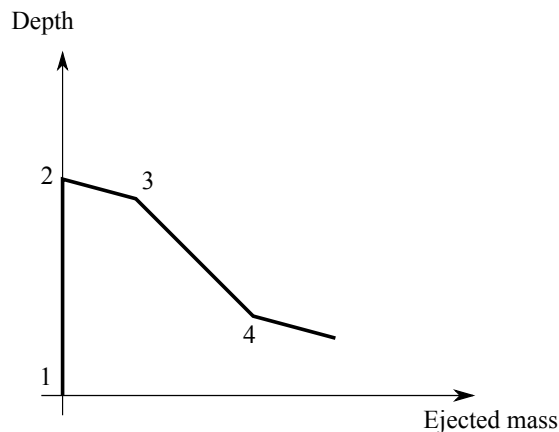

Figure 3.2: *Graph describing the stages of the ground stabilization process.*

In Figure 3.2 and 3.3 the procedure of drilling and ejecting mass is graphically described. The numbers in Figure 3.2 correspond to the different stages in the process. The depth of the tool is on the vertical axis and the cumulative ejected mass is on the horizontal axis. The main focus in this thesis lies between stage 3 and 4. As may be observed in Figure 3.2 the stabilization process stops before reaching ground level.

1. Commencing drilling.

2. The tool starts to rotate at a constant depth until the desired amount of mass between the end of the tool and the hose outlet has been ejected.

3. Bottom mass is ejected, rise of tool commences while still ejecting mass.

4. Valve closes and the mass left in the hose is ejected.

For different projects, different parameters are used. A typical reference value for the ejected mass per meter can be between 25-60 kg/m and a typical material mix is 50% cement and 50% limestone (Dmixab 2014-02-06).
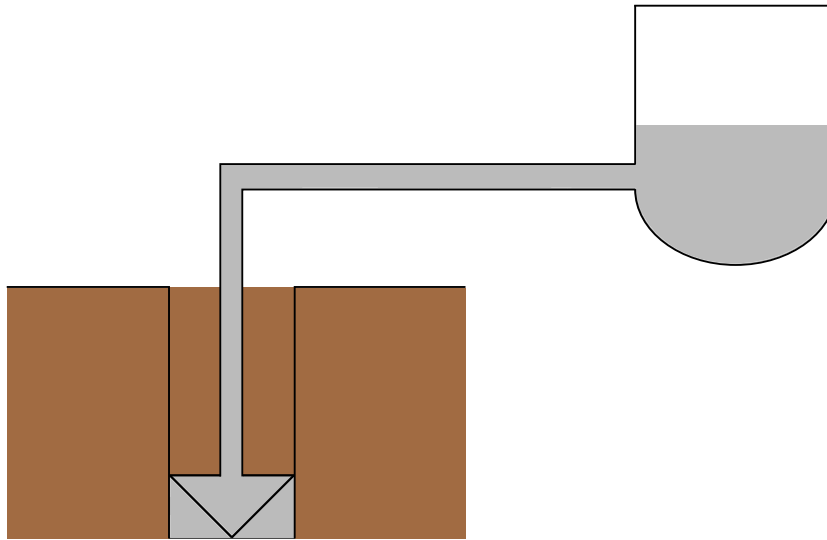
Figure 3.3: *A simplification of the process. Here the bottom mass has been ejected and the rise of the tool shall commence.*

3.2.1   Process Inputs

Input to the process is the rise speed of the tool. The rise speed is set by sending a dimensionless integer from a SCADA system to a PLC which in turn sets the rise speed. The pressure in the tank is set before the stabilization commences but not changed during runtime. Furthermore, there is a valve, controlling the flow from the tank, which is either open or closed. The rotational speed of the drilling tool is set before commencing the process.

3.2.2   Process Outputs

Measured outputs in the process are the mass of the material tank, the depth of the tool, the rotational speed of the tool, pressure in tank and pressure in hose. These measurements are sampled two times every second, $T_s = 0.5$ s. Resolutions for the measurements are *1 kg*, *0.01 m*, *1 rpm* and *0.1 bar* respectively. Data holding tank mass and depth are logged and saved in a database. Figure 3.4 displays data from a real process with a nominal ejected mass per meter of 60 kg/m.
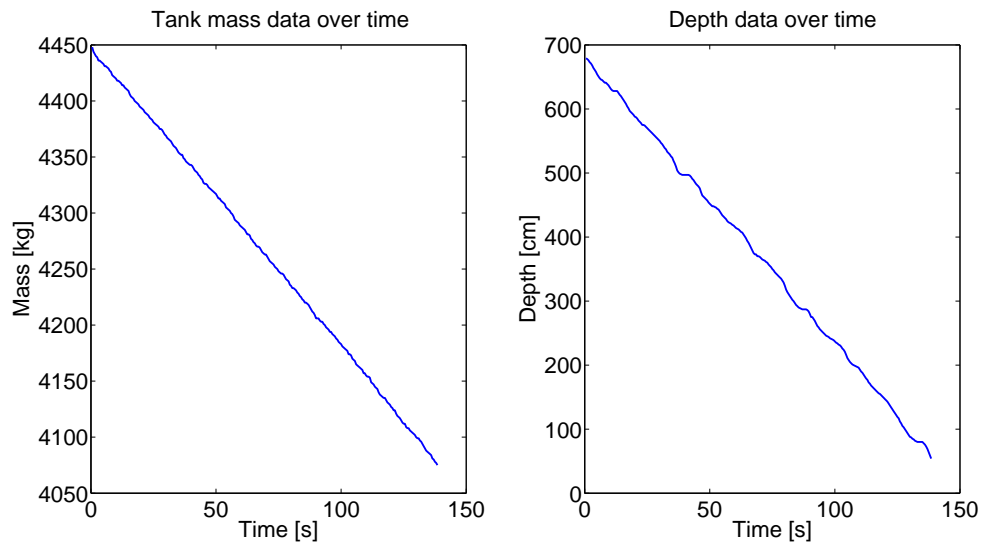
Figure 3.4: *Data collected from the real process. The starting time is when the bottom mass has been ejected and the tool is rising while material is ejected.*

3.2.3 User Interface

When running the process, a user interface is visible for the operator. It contains a graph which displays the depth of the drilled hole on the vertical axis, $[m]$, and the estimated ejected mass per meter on the horizontal axis, $[kg/m]$. Data collected by a PLC is logged to an SQL Server-database via a SCADA system.
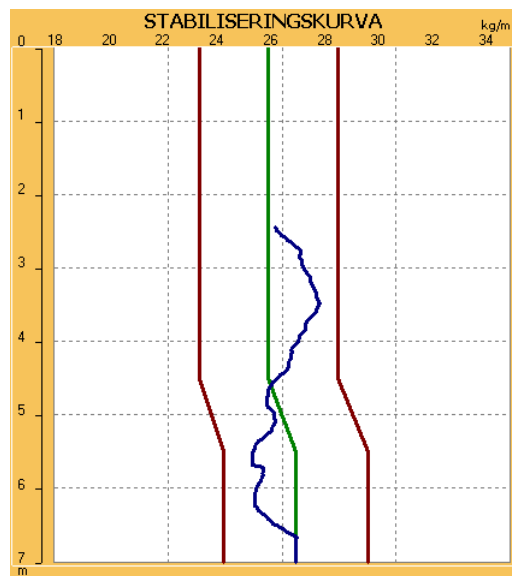
Figure 3.5: *An example of a graph visible during runtime.*

The graph visible for the operator during runtime typically looks like the one in Figure 3.5. In the graph the green line represents the desired value for the amount of material ejected per meter and the blue line represents the estimated ejected mass per meter calculated from measurements. The red lines are the tolerance levels, typically $\pm 10\%$ of the reference value.

3.2.4   Current Methods of Disturbance Rejection and Control

Since the goal is to improve the disturbance rejection and control of the process, the current methods used for this are described here. These methods are further discussed in chapters 5 and 6.

Disturbance rejection   Currently, moving average filters are used both for estimating the ejected mass per meter and for disturbance rejection of the quantity. A moving average filter is a type of FIR-filter. The algorithm replaces the data points with an average of a data series and moves the span for the data series forward. This method is typically used in economics to smoothen data enough to distinguish different features (Everitt 2002). Before using the moving average filter, the blue line in Figure 3.5 was fluctuating substantially.

Automatic control   There is also a function implemented for automatic stabilization which checks if the estimated average mass per meter exceeded or fall below a certain tolerance level and changes the rise speed in discrete steps depending on in which range the error difference is.

4   Modeling

In this chapter, mathematical modeling of the ground stabilization process is presented. The ground stabilization process includes some parts which are complicated to model, therefore some approximations and assumptions are made. These are also presented here. This chapter focuses on setting up differential equations for the process and forming a state space model.

4.1   Assumptions and Approximations

The complexity of the process makes the process difficult to model without certain assumptions and approximations. The following assumptions have been made:

- **Incompressible fluid** - The material is assumed to be an incompressible fluid.

- **Material distribution** - It is assumed that when the process is running, the mass in the hose is constant and uniformly distributed over the entire length of the hose.

- **Starting time** - When setting up the equations for the process, the starting time is defined to be the time when the bottom mass has been ejected and the rise of the tool is commencing. This is done since this is the part of the process which is automatically controlled.

4.2   The Model

Two important outputs from the process are the position of the hose outlet and the amount of mass ejected. The position and the ejected mass may be used to estimate the amount of mass ejected per meter which is the quantity of greatest interest in the process. Lets first consider the position of the hose outlet.
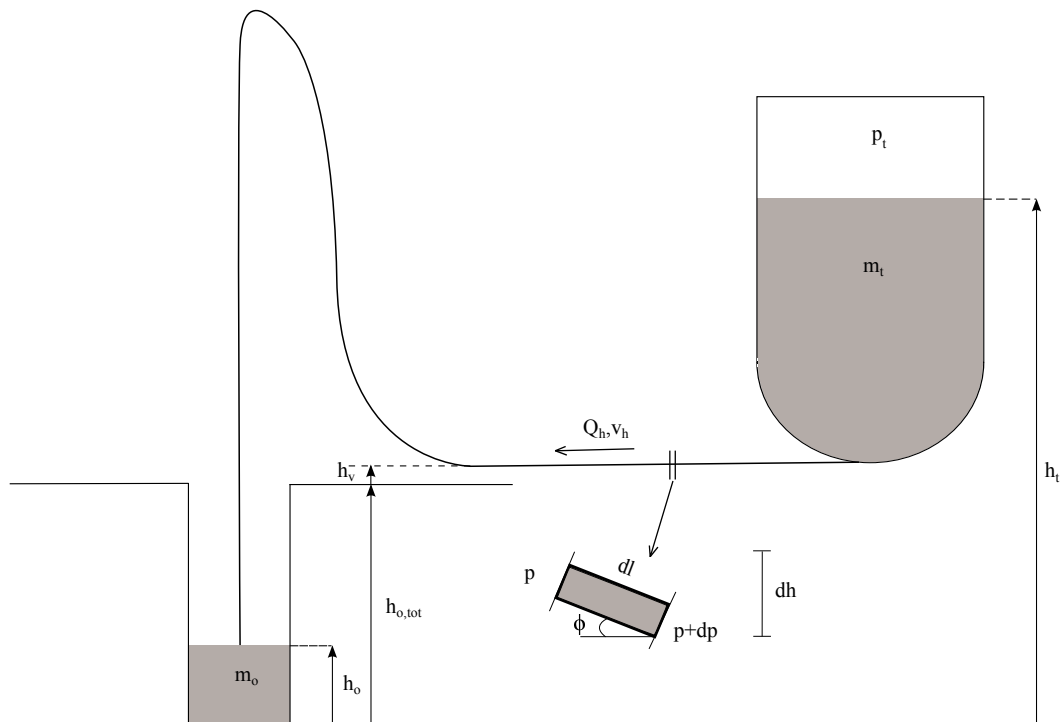
Figure 4.1: *Tank and hose with variables explaining the pressures, masses and flow.*

Hose outlet position   The position of the hose outlet plays a big part of the model. The position is indirectly controlled when controlling the rise speed. See Figure 4.2, where the position of the tool is defined graphically.
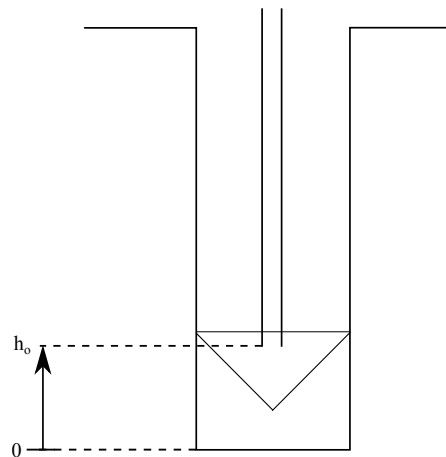

Figure 4.2: *Coordinate system for the position of the hose outlet.*

By defining the coordinate system according to Figure 4.2, the starting position is zero. If defining the starting time as when the mass in the bottom has been ejected and the rise of the tool commences, the initial condition $h_o(0) = 0$ is obtained. This

yields a simple relation between the hose outlet position and the rise speed

$$\dot{h}_o(t) = v(t) \tag{4.1}$$

Pressure, Flow and Mass The pressure difference and flow in the hose are parameters that determine the rate at which the mass is ejected. In Figure 4.1 the process is described where variables for the tank, hose and outlet have subscripts t,h and o respectively. There is a pressure difference in the hose giving rise to a flow of material. The material flow is subject to a resistance in the form of friction in the hose. First, consider a small piece of the hose, see Figure 4.3.
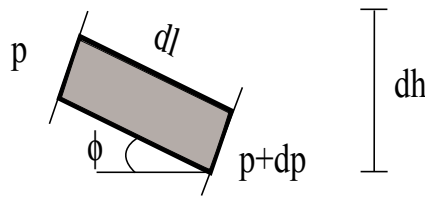
Figure 4.3: *Small piece of the hose with length dl, height difference dh and pressure difference dp.*

In Figure 4.3, dl is the length, dh is the height difference, ϕ is the tilt angle and dp is the pressure difference between the ends of that small piece of hose. By forming Newton's second law for this small piece, the following balance equation is obtained.

$$\rho A_h \dot{v}_h dl = A_h dp - \rho A_h dl g \sin\phi - A_h dR_h v_h A_h \tag{4.2}$$

Here, ρ is the density of the material, A_h is the cross sectional area of the hose, R_h is the flow resistance constant in the hose and $\dot{v}_h$ is the acceleration of the material in the hose. The friction between the walls of the hose and the material adds a resistive element which can be considered proportional to the flow. This gives rise to a pressure difference (Ljung and Glad 1994).

$$p_{fric} = R_h Q_h(t) \tag{4.3}$$

Integrating Equation 4.2 over the length of the hose yields

$$\rho l_h \dot{Q}_h(t) = A_h p_h + \rho A_h g(h_t(t) - h_o(t)) - A_h R_h Q_h(t) \tag{4.4}$$

where $h_t(t)$ is the distance between the bottom of the drilled hole and the surface level of the material in the tank. The term

$$\rho A_h g(h_t(t) - h_o(t))$$

arises from the gravitational force from the material in the hose between the surface level of the tank and the depth of the hose outlet. By dividing with the density and hose length, the differential flow equation can be written as

$$\dot{Q}_h(t) = \frac{A_h}{\rho l_h} p_h + \frac{A_h g}{l_h}(h_t(t) - h_o(t)) - \frac{A_h R_h}{\rho l_h} Q_h(t) \tag{4.5}$$

The distance, $h_t(t)$, depends on the material level in tank as well as the total drilled depth, $h_{o,tot}$, and the height of the vehicle carrying the material tank, h_v. This can be expressed as

$$h_t(t) = h_{o,tot} + h_v + \frac{1}{\rho A_t} m_t(t) \qquad (4.6)$$

where A_t is the cross sectional area of the material tank and h_v is the height of the vehicle carrying the material tank. Note that the material tank here is assumed to have constant cross sectional area which is an approximation. The relation between the pressure in the tank and the pressure difference in the hose can be derived using Bernoulli's equation. Here, a simplification has been made assuming that the height difference between the material in the tank and the hose is small enough to neglect. The relationship can then be written as

$$p_t + \frac{1}{2}\rho \dot{h}_t^2 = p_h + \frac{1}{2}\rho v_h^2 \qquad (4.7)$$

The flow caused by the height difference between the bottom of the drilled hole and the bottom of the tank, $Q_{h,0}$, can be calculated by setting $\dot{Q}_h = p_h = m_t = h_o = 0$.

$$Q_{h,0} = \frac{\rho g}{R_h}(h_{o,tot} + h_v) \qquad (4.8)$$

The total mass in the system is constant which implies that there must be a balance between the mass in the tank, the mass in the hose and the ejected mass. The balance equation can be written as

$$m_t(t) = M_t - \rho A_h l_h - m_o(t) \qquad (4.9)$$

where M_t is the starting mass in the tank and m_o is the ejected mass. The rate in which the mass is ejected is proportional to the flow in the hose

$$\dot{m}_o(t) = \rho Q_h(t) \qquad (4.10)$$

4.3   Model evaluation

Before moving on to forming a state space model of the process the model needs to be analyzed. The position of the hose outlet has one big contribution from the rise speed. The only other factor to consider here is measurement disturbances on the signal which may be studied in raw data measurements.

Studying Equation 4.5, three contributions to the time rate of change of the flow can be observed. The magnitude of the first term, involving the pressure difference, is estimated to be in the order of

$$\frac{A_h}{\rho l_h} p_h \approx \frac{0.011}{300 * 60} 5 * 10^5 \approx 0.3$$

Now consider the second term concerning the flow caused by the height difference. The contribution is approximately in the order of

$$\frac{A_h g}{l_h}(h_t(t) - h_o(t)) \approx \frac{0.011 * 9.81}{60}10 \approx 0.002$$

By differentiating a time series containing depth data, a time series containing rise speed is attained. The average rise speed, $v_{app} = 0.04$ m/s, of the time series together with the nominal amount of mass ejected per meter and density, is used to calculate an approximate value for the flow during the process, $Q_{h,app} = 0.008$ m^3/s. The flow resistance constant can be approximated to be in the order of

$$R_h \approx \frac{p_h}{Q_{h,app}} \approx \frac{5 * 10^5}{0.008} \approx 6.25 * 10^7$$

The contribution from the resistive term is approximated to be in the order of

$$\frac{A_h R_h}{\rho l_h}Q_{h,app} \approx \frac{0.011 * 6.25 * 10^7}{300 * 60} * 0.008 \approx 0.25$$

In the raw data plot of the tank mass in Figure 3.4 in Chapter 3 a quite even flow of material can be observed. This implies that the contribution from the height difference is very small since the flow rate should decrease as the hose outlet rises. This is also supported by the approximations made above. This motivates that this term can be neglected in the state space model.

By studying Equation 4.7 it can be observed that if the velocity of the material in the hose is higher than the rate at which the surface level in the tank is decreasing, the pressure must be higher in the tank than in the hose. This coincides with the information supplied by Dmixab. Approximate values of the parameters used in the model can be found in Table 4.1.

Parameter	Value	Comment
A_h	0.011 m^2	Known.
A_t	$\sim$ 1.7 m^2	Calculated from a rough estimate of the diameter.
$h_{o,tot}$	7-20 m	Known. Varies between different projects.
h_v	$\sim$ 1 m	Rough approximation.
l_h	$\sim$ 60 m	Approximate value provided by Dmixab.
m_h	$\sim$ 17 kg	Estimated from experiment conducted by Dmixab.
p_h	$\sim$ 5 bar	Parameter set before running the process, has variations but is assumed constant. Provided by the Dmixab.
R_h	$\sim 6.25*10^7$ kg/m^{4}s	Approximated using a typical pressure and flow used in the process.
ρ	$\sim$ 300 kg/m^3	Approximated using the estimated mass in the hose when it is full and the dimensions of the hose.

Table 4.1: *Parameters of the model.*

4.4   The Model on State Space Form

By choosing appropriate variables as dynamic states, a state space equation can be formed. The states are

$$\mathbf{x} = \begin{bmatrix} x_1 \\ x_2 \\ x_3 \end{bmatrix} = \begin{bmatrix} h_o \\ Q_h \\ m_t \end{bmatrix}$$

The natural choice of mass variable would be the ejected mass, m_o, since it is one of the interesting quantities, but the mass in the tank, m_t, is used since it is a measured quantity. The pressure difference in the hose is modeled as a constant. The rise speed is input to the model

$$u = v$$

which is the only manipulated variable during the procedure. In the previous section it was established that the height difference had low influence on the time rate of change of the flow which simplifies the dynamic flow equation. Solving for the derivatives of the state variables yields the following dynamic equations:

$$\dot{x}_1 = u$$
$$\dot{x}_2 = -\frac{A_h R_h}{\rho l_h} x_2 + \frac{A_h}{\rho l_h} p_h$$
$$\dot{x}_3 = -\rho x_2$$

The starting mass in the tank minus the mass in the hose when the process starts serves as initial condition on the third state. The dynamical state space equation can then be written on matrix form as

$$\dot{\mathbf{x}} = \begin{bmatrix} 0 & 0 & 0 \\ 0 & -\frac{A_h R_h}{\rho l_h} & 0 \\ 0 & -\rho & 0 \end{bmatrix} \mathbf{x} + \begin{bmatrix} 1 \\ 0 \\ 0 \end{bmatrix} u + \begin{bmatrix} 0 \\ \frac{A_h}{\rho l_h} \\ 0 \end{bmatrix} p_h \tag{4.11}$$

with the initial conditions

$$\mathbf{x}(0) = \begin{bmatrix} 0 \\ 0 \\ M_t - \rho A_h l_h \end{bmatrix}$$

The output equation is

$$\mathbf{y} = \begin{bmatrix} 1 & 0 & 0 \\ 0 & 0 & 1 \end{bmatrix} \mathbf{x} + \begin{bmatrix} 1 & 0 \\ 0 & 1 \end{bmatrix} \mathbf{d} \tag{4.12}$$

where $\mathbf{d}$ is a vector containing disturbances on the outputs. The true output of the system though, is the ejected mass per meter

$$y = \rho \frac{Q_h}{v} = \rho \frac{x_2}{u}$$

which introduces a nonlinearity. Note that the flow is not a measured signal which implies that an observer needs to constructed.

4.5   Controllability and Observability

The system above is written on the form

$$\dot{\mathbf{x}} = \mathbf{A}\mathbf{x} + \mathbf{B}\mathbf{u}$$
$$\mathbf{y} = \mathbf{C}\mathbf{x} + \mathbf{D}\mathbf{u}$$

where in this case, $\mathbf{D} = 0$. To make sure that the system can be controlled, the rank of the controllability matrix of the system is investigated. The controllability matrix is constructed from the $\mathbf{A}$ and $\mathbf{B}$ matrices as

$$\mathbf{CO} = \begin{bmatrix} \mathbf{B} & \mathbf{AB} & \mathbf{A}^2\mathbf{B} & \dots & \mathbf{A}^{n-1}\mathbf{B} \end{bmatrix} \tag{4.13}$$

where n is the number of states. The condition for controllability is that $rank(\mathbf{CO}) = n$. Similarly to the controllability check, it is possible to construct an observability matrix from the $\mathbf{A}$ and $\mathbf{C}$ matrices as

$$\mathbf{OB} = \begin{bmatrix} \mathbf{C} \\ \mathbf{CA} \\ \mathbf{CA}^2 \\ \vdots \\ \mathbf{CA}^{n-1} \end{bmatrix} \tag{4.14}$$

and the condition for observability is that $rank(\mathbf{OB}) = n$ (Egardt 2013). Performing the controllability and observability check on the state space model derived in this chapter results in

$$rank(\mathbf{OB}) = 3$$
$$rank(\mathbf{CO}) = 3$$

which shows that the system is both observable and controllable since there are three dynamic states in the model.

5 Filter Design

In this chapter, methods of filtering the signals of interest are investigated, compared and simulated. This includes estimation of flow, estimation of ejected mass per meter, first order low pass filtering, FIR low pass and FIR differentiator filters.

5.1 Estimating the Flow

Mass and hose outlet position are measured but the second state in the state space model, representing the flow, is not. Therefore an observer is constructed. The observer is constructed using the `place()`-function in MATLAB which optimizes the choice of eigenvectors in order to have a robust solution. The function utilizes the $\mathbf{A}$ and $\mathbf{C}$ matrices from the state space model along with the desired pole placement of the closed loop system as input when calculating the observer gain, $\mathbf{L}$. With an estimated state vector an estimated output is obtained as

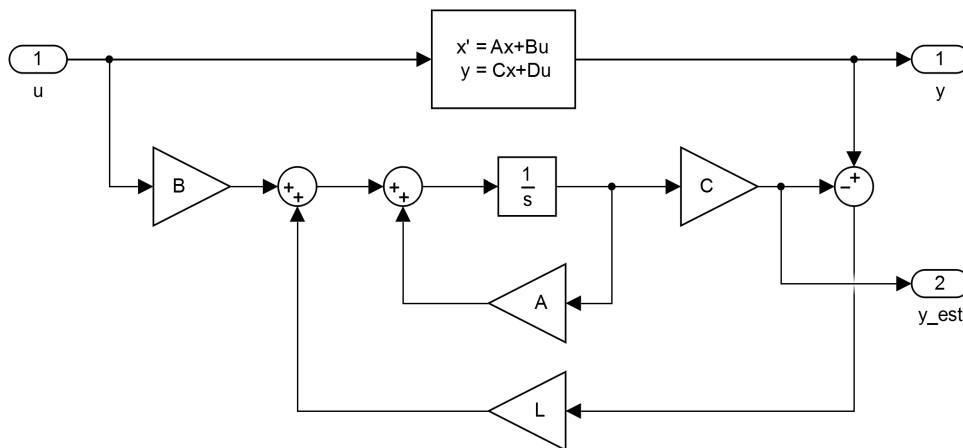$$\hat{\mathbf{y}}(t) = \mathbf{C}\hat{\mathbf{x}}(t) \tag{5.1}$$

When the true output differs from the estimated output, the estimate has to be corrected according to the correction factor

$$\mathbf{y}(t) - \hat{\mathbf{y}}(t) = \mathbf{y}(t) - \mathbf{C}\hat{\mathbf{x}}(t) \tag{5.2}$$

Multiplying the correction factor with an observer gain yields the observer

$$\dot{\hat{\mathbf{x}}}(t) = \mathbf{A}\hat{\mathbf{x}}(t) + \mathbf{B}\mathbf{u}(t) + \mathbf{L}(\mathbf{y}(t) - \mathbf{C}\hat{\mathbf{x}}(t)) \tag{5.3}$$

Figure 5.1: *Block diagram of a state space model with an observer.*

In Figure 5.1 the observer is implemented with the model of the system, assuming perfect knowledge of the system. In the figure, L is the observer gain designed with the `place()`-function.

The quantity of interest in the process is the amount of mass ejected per meter. From the relations described in Chapter 4, this quantity can be written as

$$X = \frac{dm_o}{dh_o} = \rho \frac{Q_h}{v} \tag{5.4}$$

Henceforth, mass ejected per meter will be denoted by X. By using the input velocity which is assumed measured as well as the estimated flow, X can be calculated as

$$X = \rho \frac{\hat{Q}_h}{v} \tag{5.5}$$

Simulation   A simulation was performed to observe the estimated ejected mass per meter using the estimated flow and rise speed. The simulation was performed in Simulink using the state space model and an observer. The rise speed is not measured on the real process. However during this simulation rise speed, obtained by differentiating depth data from the real process, is used. Differentiation creates a time series, see Figure 5.2. At some points the rise speed was zero which would cause the simulation to crash due to division by zero. This was solved by holding the previous value at those points.
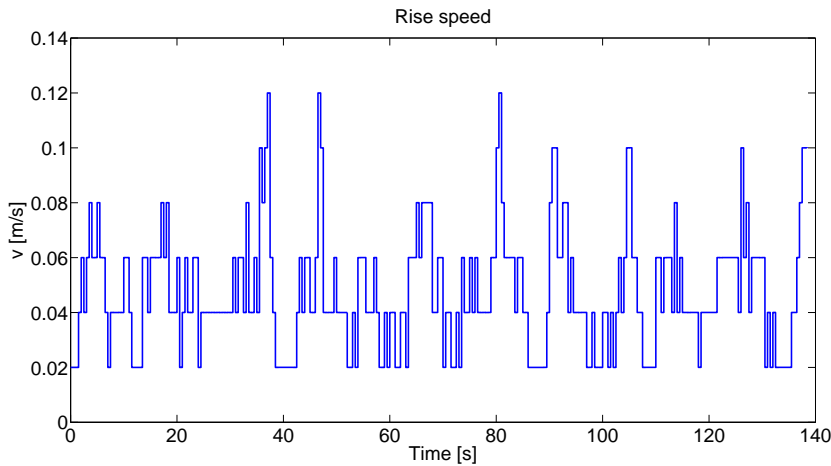
Figure 5.2: *Plot of time series used as input to simulation(rise speed).*

As can be observed from the figure above, the resulting signal is greatly quantized. This is most probably due to the relatively low resolution of the depth measurements which the velocity signal was differentiated from. The pressure was set constant at 2.5 bar during the simulation. On the tank mass signal, a band-limited white noise was added to simulate measurement disturbances. The noise power was tuned until

it resembled the noise observed in raw data of the tank mass. In Figure 5.3, the resulting estimated ejected mass per meter, risen distance, tank mass and observed flow is displayed.
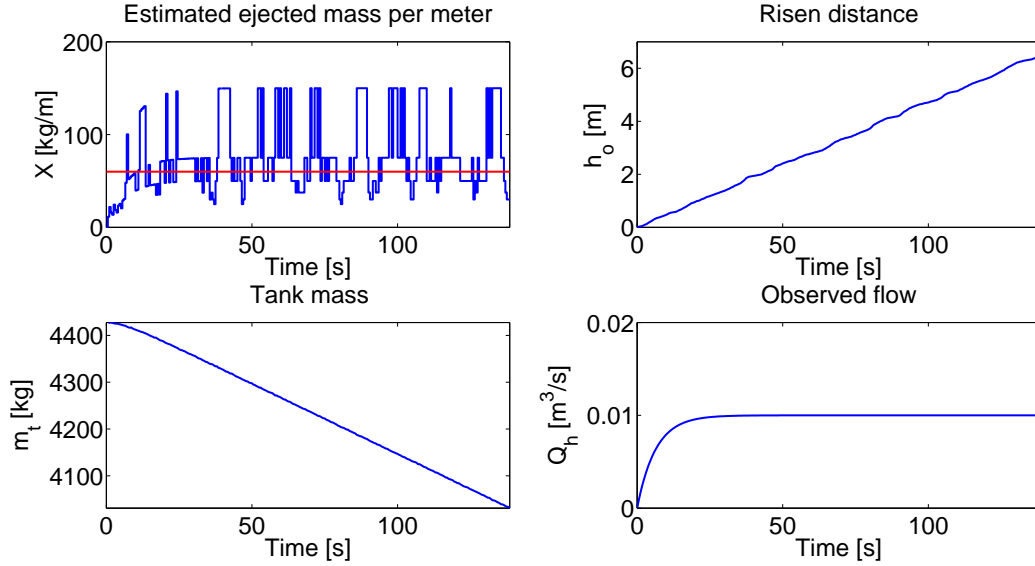
Figure 5.3: *Plots displaying estimated ejected mass per meter, risen distance, tank mass and observed flow from a simulation.*

The nominal value when collecting the depth data used to calculate the input is 60 kg/m. The red line in the first plot in Figure 5.3 displays this value. It can be observed that when having a constant pressure of 2.5 bar the estimated ejected mass per meter revolves around the nominal value, although having large fluctuations. What can also be observed is that the rise speed is very noisy and the observed flow is not noisy at all. The depth data which the rise speed was calculated from was noisy and differentiation is very noise sensitive. In the simplified state space model, the terms where the flow is dependent on the tank mass and depth was considered small enough to be neglected. This means that the flow is not subject to disturbances in the model. This can be observed in the figure.

5.2 First Order Low Pass Filter

The first order low pass filter in its discrete form can be expressed according to Equation 5.6 where y_f is the filtered signal, y is the original signal and α is a filter constant.

$$y_f(n) = \alpha y(n) + (1 - \alpha)y_f(n - 1) \tag{5.6}$$

The first order low pass filter is a weighted sum of the current signal and the previous filtered signal. How much weight put on the two is determined by the filter constant,

α. The equation can be rewritten as

$$y_f(n) = y_f(n-1) + \alpha(y(n) - y_f(n-1)) \tag{5.7}$$

and from here it is straightforward to see that the filter output change is proportional to the difference between the current unfiltered signal and the previous filtered signal. The first order low pass filter is an infinite-impulse-response(IIR) filter with a single pole.

Ramp offset   The material mass in the tank and the risen distance are signals which are expected to change approximately linearly over time forming ramp signals. Low pass filtering these signals according to Equation 5.6 yields an asymptotic offset in the output of the filter. This can be shown by studying the final value of the difference between the output and the input to the filter. When transforming the filter into the $\mathcal{Z}$-domain the following transfer function is obtained.

$$F_{LP}(z) = \frac{\alpha z}{z - 1 + \alpha} \tag{5.8}$$

The ramp function in the $\mathcal{Z}$-domain can be written as

$$Y(z) = \frac{z}{(z-1)^2} \tag{5.9}$$

Using the discrete version of the final value theorem on the difference between the output, y_f, and input y yields

$$\lim_{i \to \infty} (y_f(i) - y(i)) = \lim_{z \to 1} Y(z)(F_{LP}(z) - 1)(z - 1) \to 1 - \frac{1}{\alpha} \tag{5.10}$$

where $Y_f = F_{LP}Y$. Thus, there will be an offset of $1 - 1/\alpha$ when low pass filtering a ramp function using Equation 5.6. For a complete derivation of the offset, see Appendix A.

5.2.1   First Order Low Pass Filtering of Ejected Mass per Meter

One alternative for disturbance rejection is to lowpass filter X calculated from the flow and rise speed, assuming the rise speed is measured and the flow is estimated.

$$X_f = LP(X) = \text{LP}(\rho \frac{\hat{Q}_h}{v})$$

Benefits of filtering the estimated ejected mass per meter instead of the tank mass and depth is that this quantity is expected to behave as a constant or step function instead of a ramp function thus not yielding an asymptotic offset in the output.

$$\lim_{i \to \infty} (y_f(i) - y(i)) \to 0$$

Obviously, due to disturbances the offset will not be strictly zero.

Simulation   A simulation was performed in order to compare the filtering performance of the first order low pass filter for different filter constants. The simulation involves the state space model, estimation of the flow, calculation of the estimated ejected mass per meter and low pass filtering of the quantity. The low pass filter is implemented according to Equation 5.6. The input here is the same rise speed that was used in the previous simulation, see Figure 5.2, and the pressure is set to be 2.5 bar. Evaluated filter constants are $\alpha = 0.5, 0.1, 0.05, 0.01$. Bode plots for the filters can be studied in Figure 5.4.
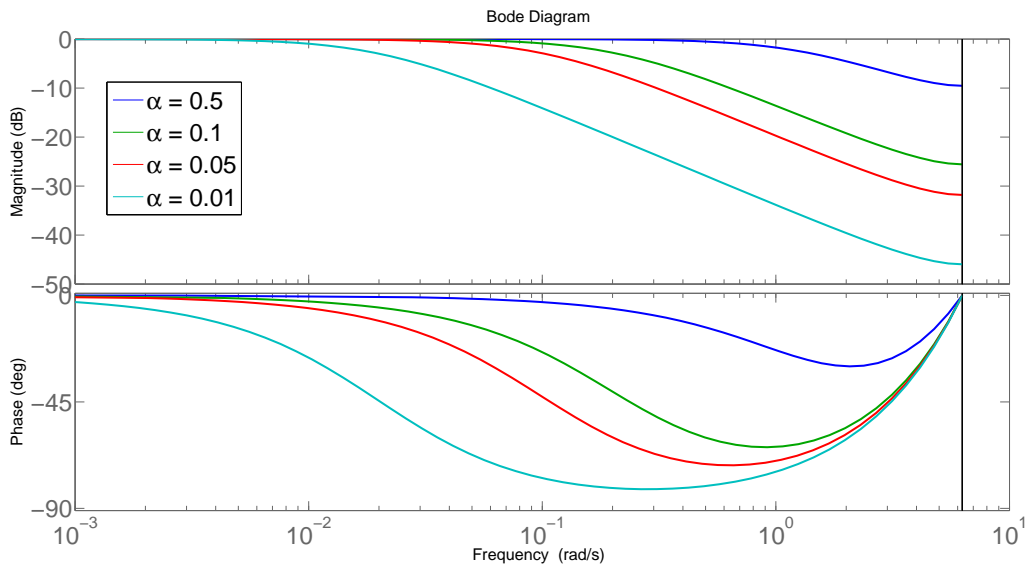
Figure 5.4: *Bode plots of low pass filters used in simulation.*

From the bode plots it can be observed that for smaller filter constants, the filtered signal will be suppressed more for lower frequencies. At the same time the signals will be subject to phase delay which will be present for lower frequencies for the filters with small filter constants. The results of the filter comparison can be studied in Figure 5.5 where the low pass filtered ejected mass per meter is plotted over time.
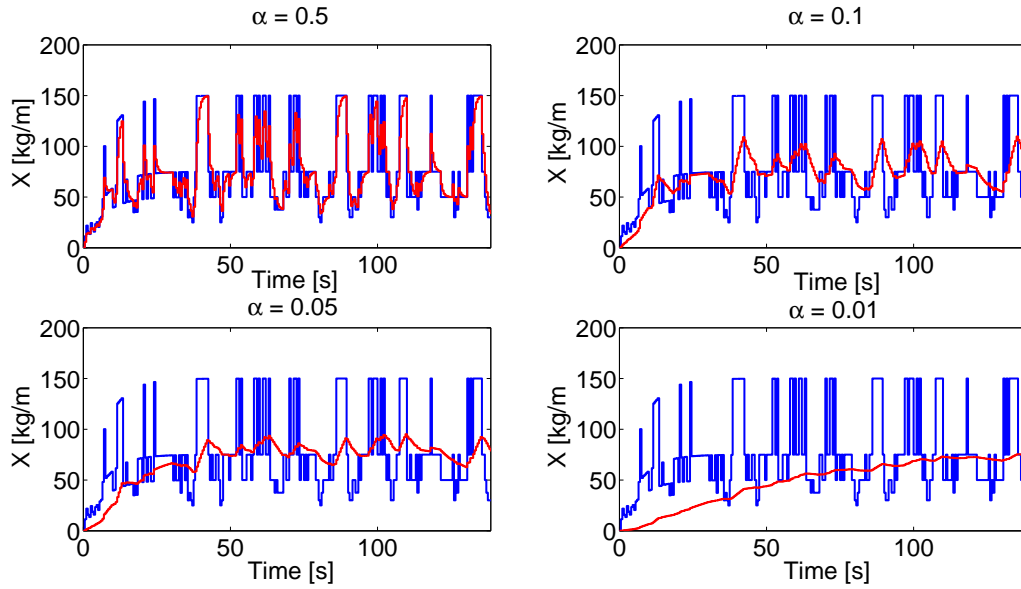
Figure 5.5: *Simulation result from filtering X comparing four filter constants. The blue line represents unfiltered values and the red line represents filtered values.*

The effect of lowering the filter constant is shown in the simulation result. For the plot in the bottom right corner the first samples, where the ejected mass per meter is still in transient phase, effect samples over a large part of the time series. A solution to this might be to start filtering when steady state is reached. At the same time, for the filter in the upper left corner which responds to changes faster, disturbance rejection is not satisfactory.

5.2.2   First Order Low Pass Filtering of Rise Speed

Instead of filtering X, the measured rise speed may be filtered before calculating X.

$$X_f = \rho \frac{\hat{Q}_h}{\mathrm{LP(v)}}$$

Simulation   Under the same simulation conditions as the previous simulation, filtering the measured rise speed before calculating the ejected mass per meter was simulated, see Figure 5.6. The results are similar, for the lowest filter constant, too much weight is put on old samples.
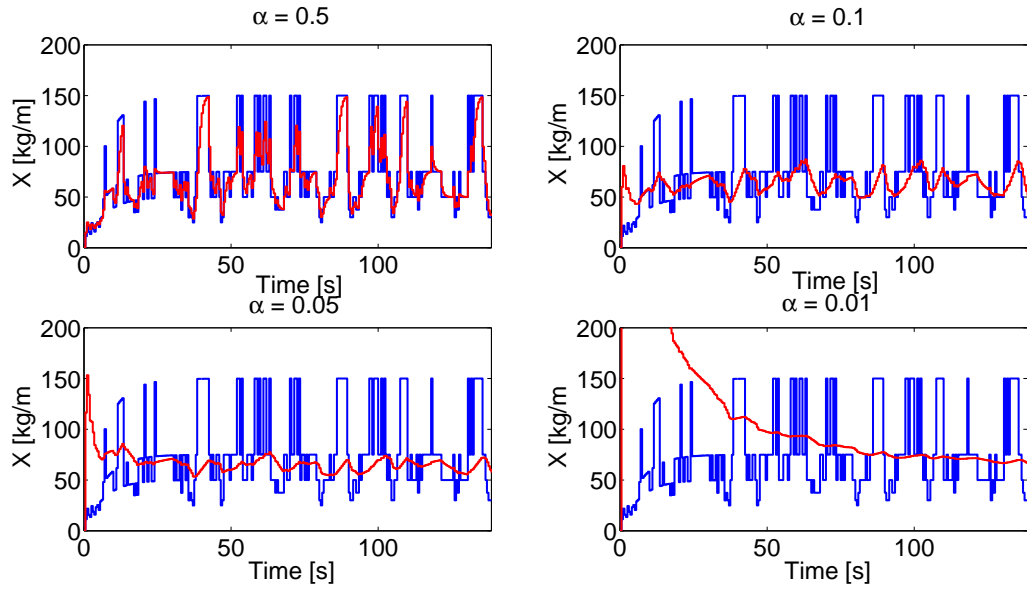
Figure 5.6: *Simulation result from filtering X comparing four filter constants. The blue line represents unfiltered values and the red line represents filtered values.*

It can be concluded, from the simulations involving low pass filtering the ejected mass per meter and the rise speed, that it does not effect the performance noticeably if filtering the rise speed before calculation instead of filtering X. What has effect on the filtering performance is the cut off frequency and phase delay which are decided by the filter constant, α. In conclusion, a compromise has to be made in order to track changes in the signal fast and at the same time suppress high frequency disturbance.

5.3   FIR Filters

Finite impulse response filters(FIR-filters) are, as the name implies, filters that have finite impulse responses. FIR-filters are commonly used in digital applications. There are two major reasons for this, one is that this type of filters are non-recursive which makes them unconditionally stable. The other reason is that they can be designed with relatively low precision arithmetics (Mulgrew *et al.* 2003). How the filter operates can be analyzed by studying Equation 5.11.

$$y_f(n) = \sum_{i=0}^{N-1} a_i y(n-i) \tag{5.11}$$

Here, y_f is the output of this filter of length N. The input to the filter is y and a_i are the filter coefficients. The length affects the performance of the filter, for large N the noise level of the filtered signal is lower but on the other hand, the delay is longer. The delay of a FIR filter is $\frac{N}{2}$ if N is even and $\frac{N-1}{2}$ if N is odd.

Linear phase   All input signals to a linear phase filter are delayed with the same delay time. A constraint for having linear phase is that the coefficients are conjugate even about the filters center point. A restrictive example of a linear phase FIR-filter is a pure delay. Consider the impulse response of a delay of k samples:

$$H(z) = z^{-k} \tag{5.12}$$

The frequency response of the delay is

$$H(\omega) = \exp^{-j\omega T_s k} \tag{5.13}$$

where T_s is the sampling time. The gain and phase of this filter are

$$|H(\omega)| = 1 \tag{5.14}$$

and

$$\angle H(\omega) = -\omega T_s k \tag{5.15}$$

respectively. As can be noted from Equation 5.15 the phase is linearly proportional to the frequency. The delay filter multiplies all the input signals by 1 and delays them a time k. If the filter instead weighs the inputs differently, different frequencies can be selected (Mulgrew *et al.* 2003).

Parks-McClellan algorithm   The Parks-McClellan algorithm is an optimization technique used when designing filters. It has significantly low complexity compared to window design methods. It minimizes an error in order to approximate a desired frequency response by iterating.

$$\min_{c_n}\{\max_{\omega} |L(\omega)(H_D(\omega) - H_A(\omega))|\} \tag{5.16}$$

The obtained filter coefficients, c_n, are the values which minimizes the maximum error between the desired and actual frequency response. The weighting parameter, $L(\omega)$, provides the filter designer with the option of emphasizing some parts of the frequency response more than others (Mulgrew *et al.* 2003). This optimization technique is utilized in many applications, for example the `firpm()`-function in MATLAB.

5.3.1   FIR Filtering Ejected Mass per Meter

It was concluded in the previous section that filtering X or filtering the rise speed, v, before calculating X, did not have large effect on the filtering performance. Therefore, the focus here has been concentrated to filter X.

Simulation   The conditions for the simulation are equal to previous simulations involving first order low pass filtering. The same input data and parameters are

used. Here, the first order low pass filter algorithm is replaced with the algorithm described in Equation 5.11. Four different filters are evaluated with increasing filter order. The FIR-filters have been designed using the `firpm()`-function in MATLAB which has filter order, amplitude and desired cut-off frequency as inputs and outputs the filter coefficients which constitutes an approximation of the desired filter. Four FIR-filters of order 4, 10, 20 and 30 were evaluated. The amplitude and phase of their fast fourier transform(FFT) can be found in figures 5.7 and 5.8 respectively.
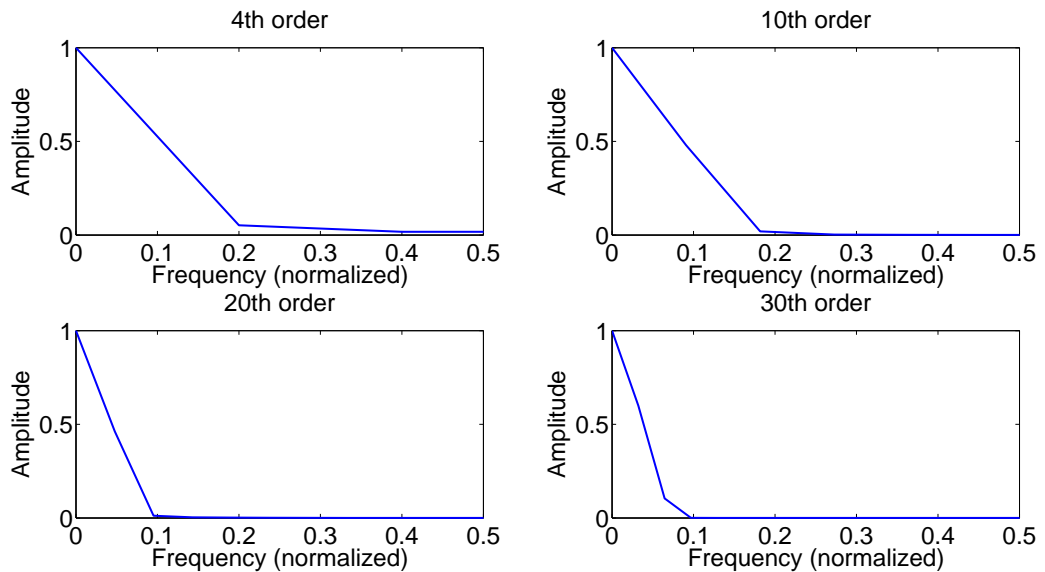

Figure 5.7: *Amplitude of the FFT of four FIR-filters.*
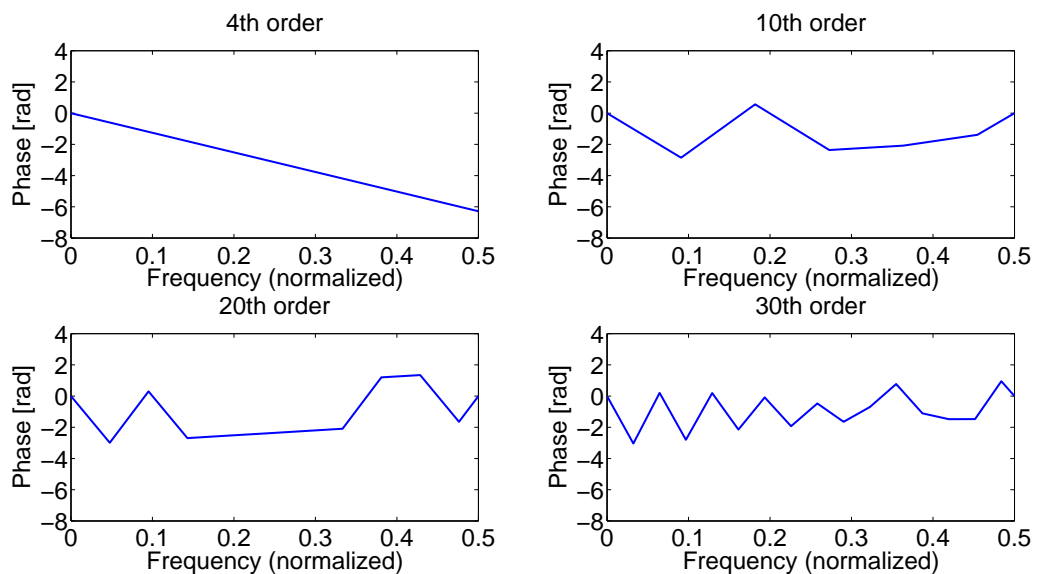
Figure 5.8: *Phase of the FFT of four FIR-filters.*

In Figure 5.9 the results of the simulation can be studied. From the plots it can be concluded that a quite high filter order is needed to suppress the disturbance on the signal. In the bottom right plot, the signal is filtered relatively well but at the same time a substantial delay is present which may cause problems when using the signal for control.
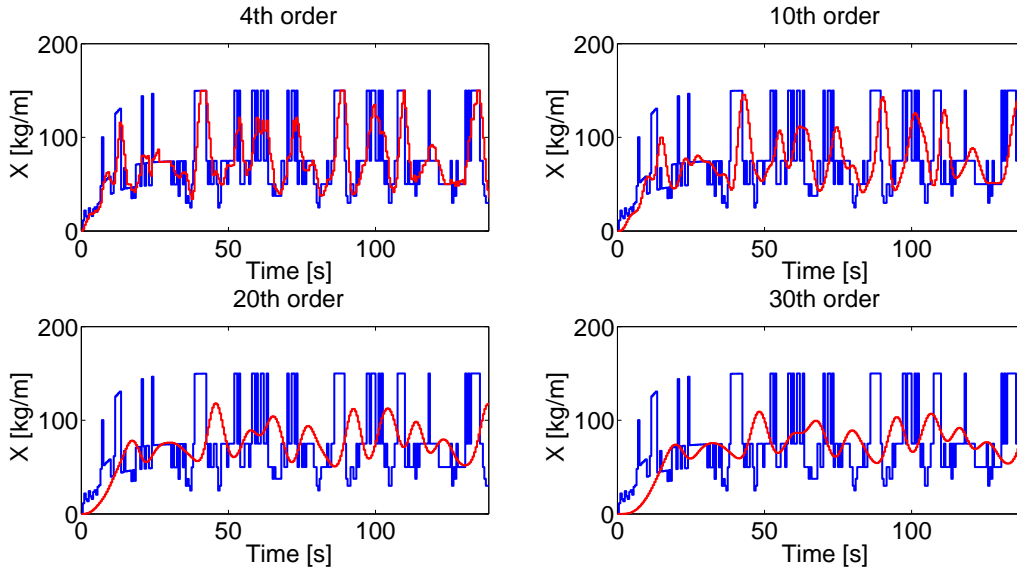
Figure 5.9: *Simulation result from filtering X comparing four FIR-filters. The blue line represents unfiltered values and the red line represents filtered values.*

5.4   Estimation Using Ejected Mass and Position

The quantity ejected mass per meter can not only be calculated using the flow and the rise speed. It may also be calculated using the time rate of change for the ejected mass and the position of the hose outlet.

$$X = \frac{dm_o}{dt} \bigg/ \frac{dh_o}{dt} = \frac{dm_o}{dh_o}$$
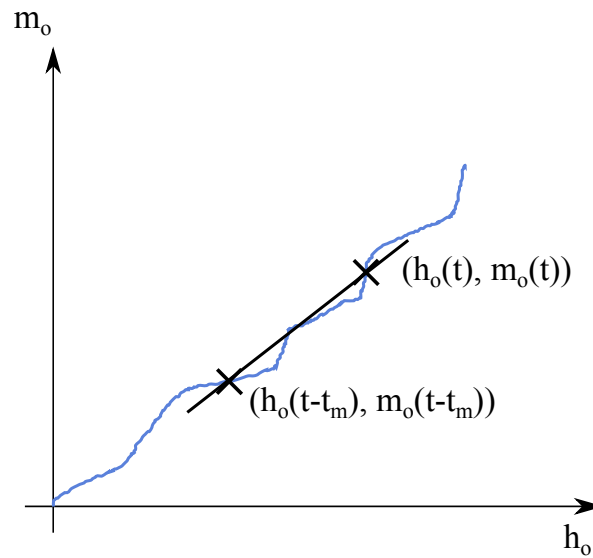
5.4.1   Moving Average

One estimation technique is to use a moving average(MA) of the mass and hose outlet position which are measured quantities. The estimation consist of a calculation of how much mass on average has been ejected over a certain length over a certain

time, and then moves the span for the average calculation, according to

$$\hat{X}(t) = \frac{m_o(t) - m_o(t - t_m)}{h_o(t) - h_o(t - t_m)} \tag{5.17}$$

where t_m is the time span used for the moving average calculation. It is an approximation of the derivative of the ejected mass divided by the risen distance. This is illustrated in Figure 5.10 where a line is drawn between the point $(h_o(t-t_m), m_o(t-t_m))$ and $(h_o(t), m_o(t))$. The slope of the line equals the estimated ejected mass per meter, $\hat{X}(t)$.

Figure 5.10: *Figure illustrating cumulative ejected mass over risen distance.*

In discrete implementation, t_m is the number of samples used for the calculation.

Simulation   A simulations was conducted comparing the moving average estimation of the ejected mass per meter using collected data and simulated data. The conditions for the simulation are a constant pressure difference of 2.5 bar and rise speed differentiated from the depth data used in this comparison. The tank mass and hose outlet depth from the simulation as well as raw data can be studied in Figure 5.11.
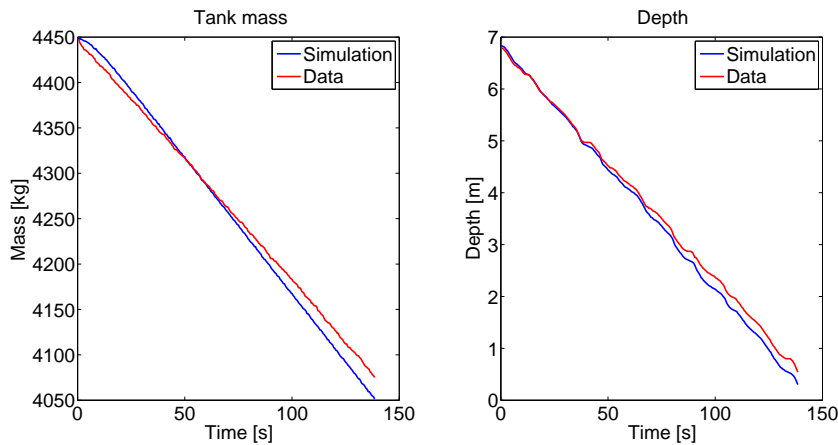
Figure 5.11: *Plots of tank mass and hose outlet depth from simulation and collected data.*

The simulation was conducted for four different time spans. In Figure 5.12 the result of the comparison can be studied. Here, the red line represents moving average estimation using data and the blue line represents simulated values.
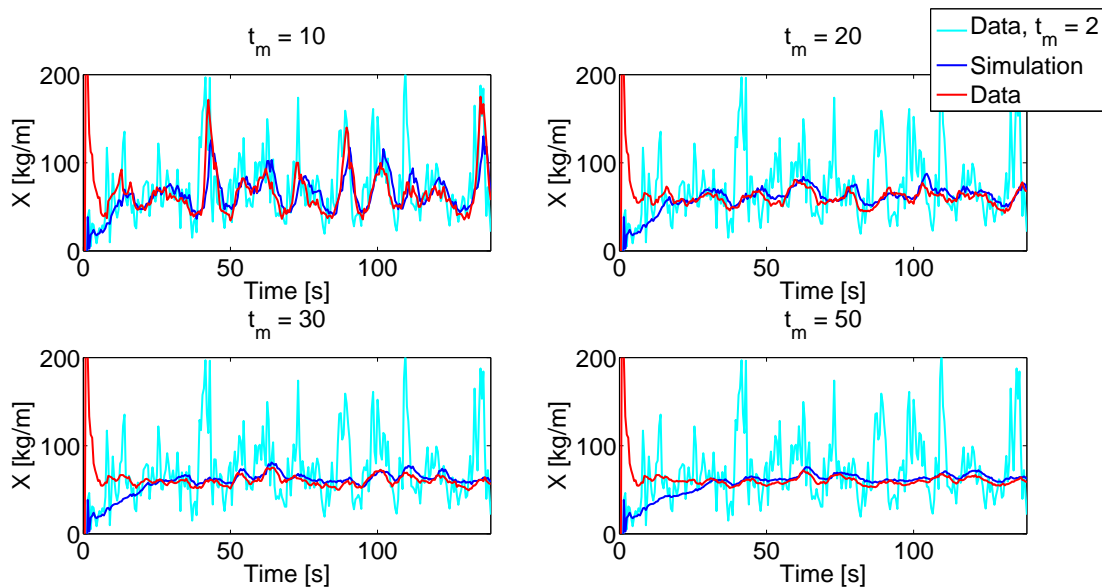
Figure 5.12: *Plots comparing the moving average estimation of the ejected mass per meter using data from the real process and simulated data. Time spans of $t_m = 10$, 20, 30 and 50 was used.*

By studying the plots, it can be observed that taking a moving average over a large time span yields an estimation less sensitive to disturbances but with a longer "warm up"-time. Since the velocity data used in the simulation was differentiated from the depth data used in the comparison, the simulated depth data should resemble the collected data which can be confirmed by studying Figure 5.11. From that figure it

can also be observed that the rate of change for the tank mass seem to be slower than for the real process in the beginning of the simulation and faster in the end. This is most probably caused by the transient behavior of the estimated flow in the simulation.

Combining MA with 1th order LP Combining the moving average estimation of X with a first order low pass filter according to Equation 5.18 and using the same simulated and collected data as above, the comparison displayed in Figure 5.13 can be studied.

$$\hat{X}_f(t) = \text{LP}(\text{MA}(X(t))) = \text{LP}\left(\frac{m_o(t) - m_o(t - t_m)}{h_o(t) - h_o(t - t_m)}\right) \tag{5.18}$$

The same time spans as in Figure 5.12 was used for this comparison. The first order low pass filter used in the simulation has a filter constant of $\alpha = 0.1$.
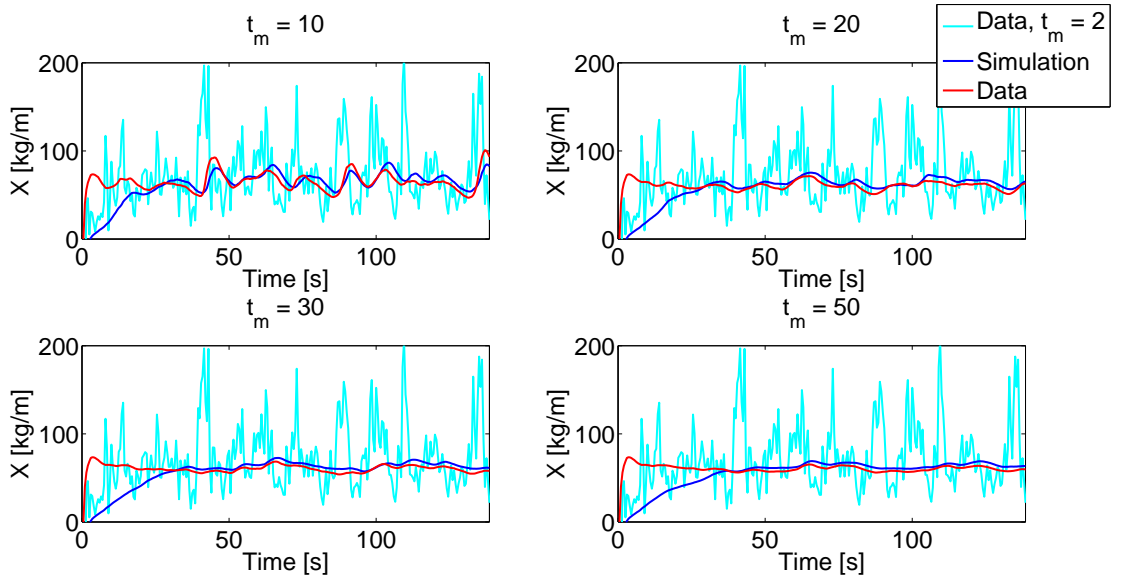
Figure 5.13: *Simulation results from an estimation of mass ejected per meter using a moving average with four different values for the time span and low pass filtering on the estimate.*

The plots in Figure 5.13 displays promising behavior even for the shorter time spans. What needs to be considered when using this estimation technique is that using a too long span for the moving average calculation will give an inaccurate estimation of the ejected mass per meter at that time.
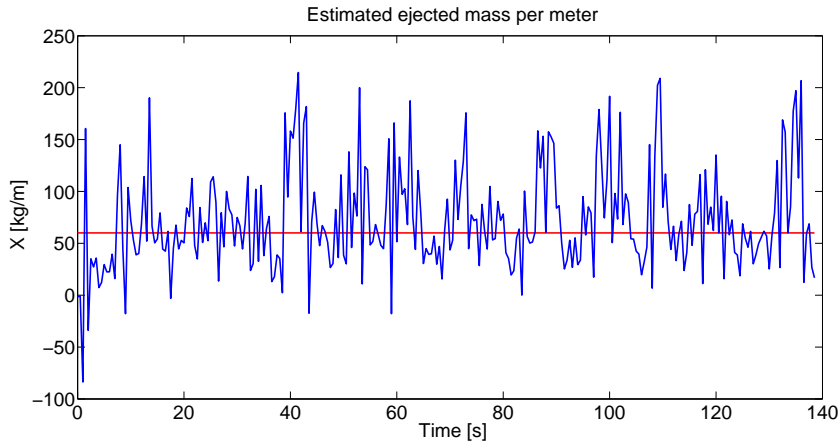
5.4.2 FIR Differentiator Filter

FIR differentiator filters are an important part of many digital applications where the rate change with respect to time needs to be acquired. Examples of usages are when

acceleration is needed from velocity data or velocity is needed from displacement data (Sheikh *et al.* 2011). A differentiator filter is often combined with a FIR low pass filter through convolution. The set-up studied in this section is a combination of two FIR-filters, one of which is a differentiator filter of order 10 and the other a low pass filter of order 30.

$$\hat{X}(t) = \frac{\text{diff}(\text{LP}(m_o))}{\text{diff}(\text{LP}(h_o))}$$

The simulation result can be observed in Figure 5.14 which is a plot of the estimated mass per meter using differentiator and low pass FIR filters on m_o and h_o. The filters were designed using the `firpm()`-function in MATLAB and for the differentiator-filter an extra argument(`firpm(..., ..., 'differentiator')`) is put in the function to declare that it should be a differentiator filter. In the simulation, the rise speed seen in Figure 5.2 was used as input to the state space model. A constant pressure difference of 2.5 bar was used.

Figure 5.14: *Simulation result of estimation of X with the use of a differentiator filter in combination with a low pass filter.*

As shown by the figure, the estimation seems to be very noisy which implies that using a differentiator filter as estimator is very noise sensitive. In figures 5.15a and 5.15b the normalized frequency responses of the differentiator filter and low pass filter are shown respectively.
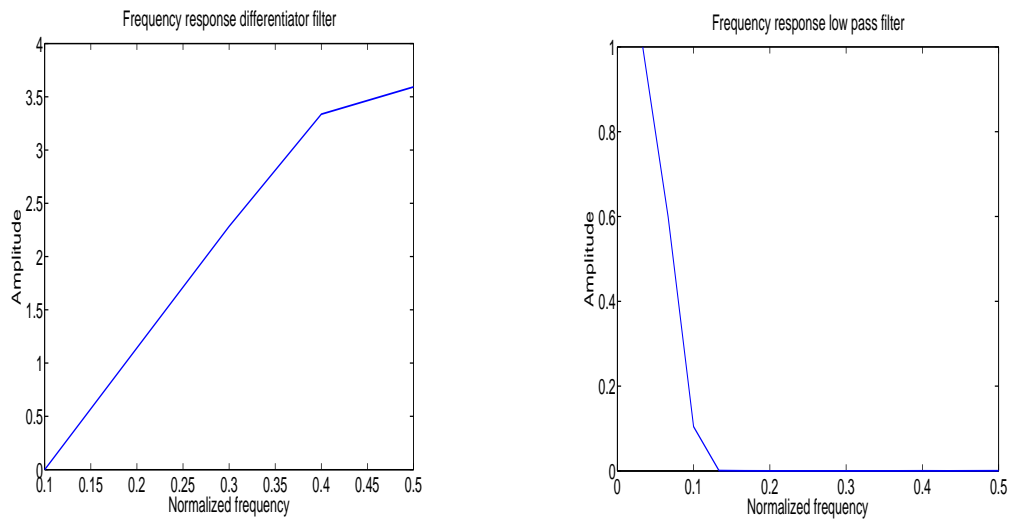
(a) Differentiator filter.

(b) Low pass filter.

Figure 5.15: *Normalized frequency responses of the differentiator filter and low pass filter used in simulation.*

6 Control Design

In this chapter a controller is designed and simulated with the mathematical model. The controller is compared to a controller using discrete steps for the control signal, which is similar to the type of control algorithm currently used for automatic control of the ground stabilization process. First a short background is given followed by the design and simulations and ending with results and comparisons.

6.1 PID-Control

PID stands for proportional integral derivative and it is straightforward to see why when studying the controller equation in the time domain.

$$u(t) = K_p e(t) + K_i \int_0^t e(\tau)d\tau + K_d \frac{de(t)}{dt} \qquad (6.1)$$

Here K_p is the proportional gain, K_i is the integral gain and K_d is the derivative gain (Lennartson 2000). The control signal and the error signal are denoted by u and e respectively. By Laplace-transformation of Equation 6.1, the transfer function of the PID-controller is obtained as

$$F_{PID}(s) = K_p + \frac{K_i}{s} + K_d s \qquad (6.2)$$

In order to realize the PID-controller in a digital application, it has to be used in its discrete form

$$u[n] = K_p e[n] + K_i \sum_{j=0}^{n} e[j]T_s + K_d \frac{e[n] - e[n-1]}{T_s} \qquad (6.3)$$

where T_s is the sampling time. Note that these terms are approximations (Lennartson 2000).

The tuning of a PID-controller, selecting the PID-parameters, is the most important part of the overall control design. Usually there is a set of specifications which should be fulfilled to achieve desired performance. The parameters do not only effect how well the reference is being tracked but also how well disturbances are being rejected and the life time of the actuator. Increasing the proportional part gives a faster but more oscillatory system, increasing the integral part will also yield a faster system but will have negative effects on the stability of the system. The derivative part has a damping effect on the system but is noise sensitive (Visioli 2014).

Normally in a physical system, there are limits on the control signal. An example is when controlling the speed of a DC-motor. If the control signal is the voltage to the motor it is safe to say that the voltage should be limited, not least for safety

reasons. See Figure 6.1 displaying a block diagram of a controller and a process. Here the control signal is limited and this is modeled as saturation.
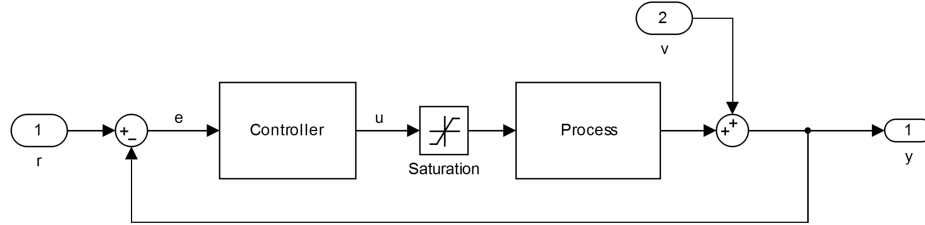
Figure 6.1: *Block diagram of a closed loop system with disturbance added on the output and saturation on the control signal.*

Since the actual control signal sent to the process is limited, the control signal depends on the unsaturated control signal and the limits as

$$u(t) = \begin{cases} u_{max} & u'(t) \geq u_{max} \\ u'(t) & u_{min} < u'(t) < u_{max} \\ u_{min} & u'(t) \leq u_{min} \end{cases} \tag{6.4}$$

where u is the control signal and u' is the unsaturated control signal. u_{max} and u_{min} are the limits for when the control signal should be saturated. Saturation introduces a non-linearity which has to be handled to have a stable system with desired performance. When the controller is saturated there is a possibility that the integral part of the controller will increase to a large value. The energy associated with this large value is later dissipated when the control signal leaves saturation. This can cause large overshoot and slow settling times (Tarbouriech *et al.* 2011). This phenomena is called wind-up since the integrator part is winding up. To overcome this problem a possible solution is to implement an anti-windup filter which feedbacks the saturated control signal via some transfer function (Lennartson 2000).

6.2 Design

There are a few parts of the system that have to be considered when designing the control system. First there is the process which is modeled with a state space representation. The actual process output used for control is an estimate involving two outputs from the model. The process output needs to be filtered due to disturbances. Then there is the controller which has to be tuned to achieve desired performance and meet the controller goals stated in Chapter 1.

6.2.1   Filter Setup

In order for the controller to act in time, the response from the process needs to be fast. This implies that a high order FIR-filter might not be suitable for filtering the process output. The setup first studied is a moving average estimation of mass ejected per meter, $\hat{X}$, which in turn is filtered with a first order low pass filter yielding a relatively fast response. This setup introduces two parameters to consider, the filter constant, α, which affects the disturbance rejection and the phase delay, and the span for the moving average estimation, t_m, which affects the accuracy of the estimation.

6.2.2   Controller Configuration

First studied is a PID-controller implemented according to Equation 6.3. The nonlinearity introduced by the estimation of the process output makes PID a suitable choice compared to, *e.g.*, LQR or linear MPC. PID-control is known to be able to compensate for disturbances and nonlinearities. The limits on the input to the process could put the system in saturation causing integrator wind-up, this is compensated for with an anti-windup filter which compares the saturated and the non-saturated control signal and feeds back a signal proportional to the difference. This configuration introduces four parameters to tune: the proportional part of the the controller, K_p, the integral part of the controller, K_i, the derivative part of the controller, K_d, and the anti-windup gain, K_{aw}. A block diagram of the system is displayed in Figure 6.2 where $\hat{X}$ is denoted with X_{est} and $\hat{X}_f$ is denoted with $X_{est,f}$.
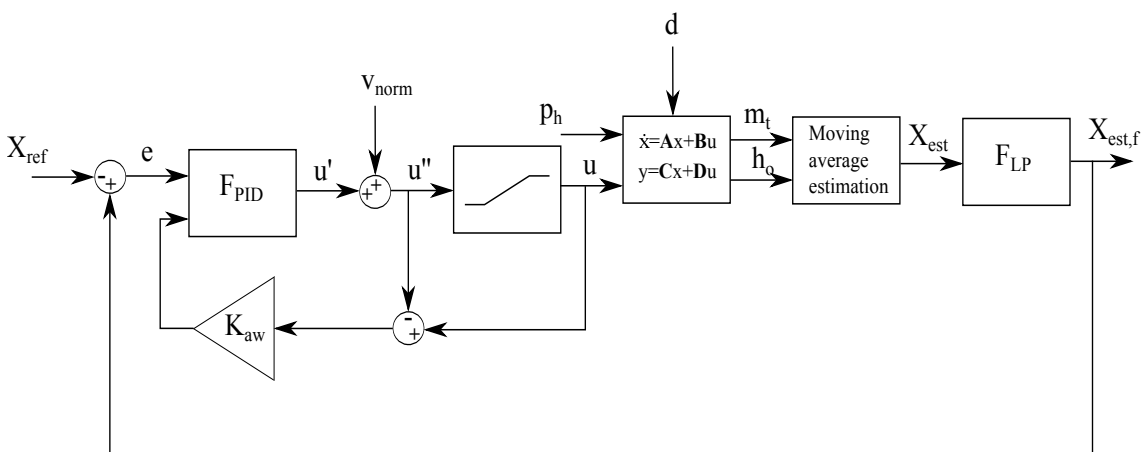

Figure 6.2: *Block diagram of the control system with anti-windup, moving average estimation of the process output and first order low pass filtering of the estimate.*

Since the rise speed should not be zero when the error is zero and the rise speed should decrease but not be negative when the error is negative, an offset, V_{norm}, is added to the control signal. The value to use as normal speed depends on the reference value.

As can be observed in the block diagram above, the reference value, X_{ref}, is subtracted and the controller has positive feedback from the filtered process output. This is due to the fact that if the estimated process output exceeds the reference value, there will be a positive error(there is too much mass ejected per meter) and a positive speed should be added to the offset.

Simulation   Simulating this setup yields the result seen in Figure 6.3 where the estimated process output, risen distance, tank mass and control speed are plotted over time. The simulation is set to stop when the hose outlet has risen 6.5 m. The reference value for the simulation is 60 kg/m and the moving average span is 10 samples. The pressure difference is set to be 2.5 bar. The normal speed is set to 0.04 m/s throughout this chapter. The normal speed was calculated using the average value of a time series of speeds differentiated from depth data. The depth data was collected from a run where the reference value was 60 kg/m. Band limited white noise is added on the tank mass and hose outlet position to simulate disturbances. For further explanation of the conditions for the simulation, see Appendix B.
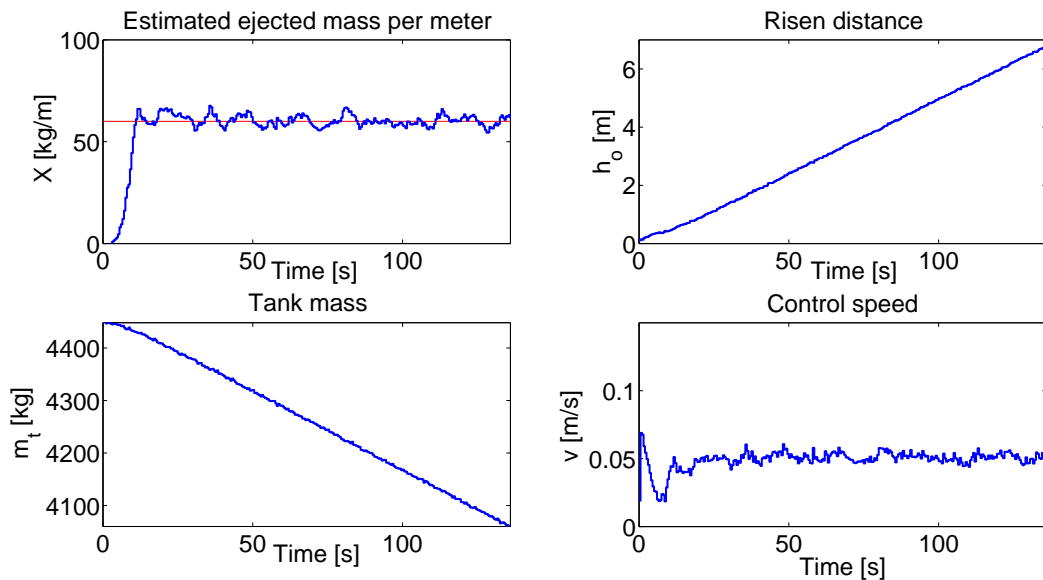
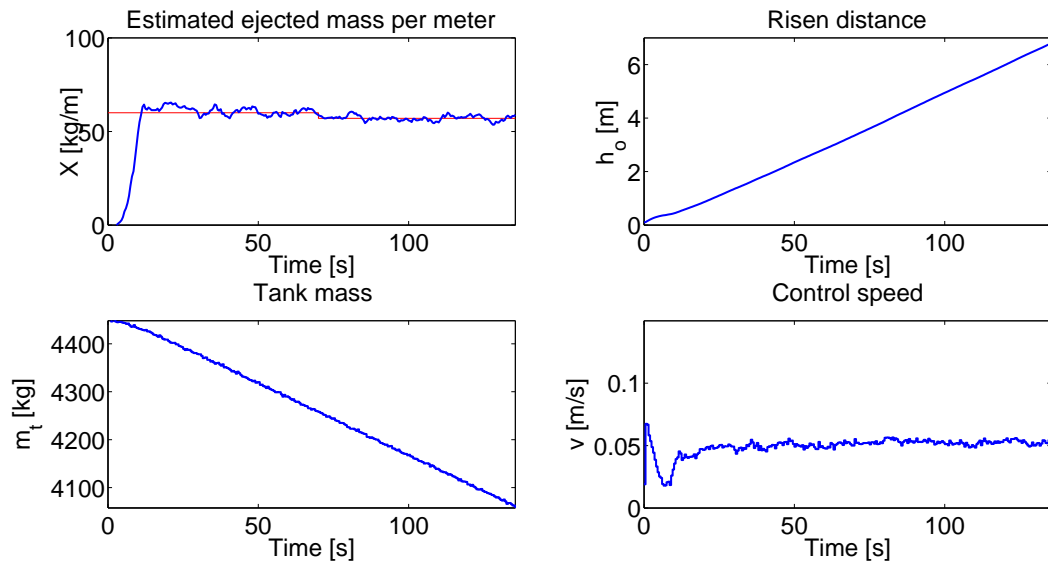**Figure 6.3:** *Simulation results of an automatically controlled ground stabilization.*

The plot in the left top corner of Figure 6.3 shows the estimated ejected mass per meter(blue line) tracking the reference value(red line). What is also visible in the

figure is the position of the hose outlet, the tank mass and the control speed. To show how the operator supervises the procedure, the estimated ejected mass per meter is plotted versus depth of hose outlet, see Figure 6.4. Parameters used in the simulation can be found in Table C.1 in Appendix C.
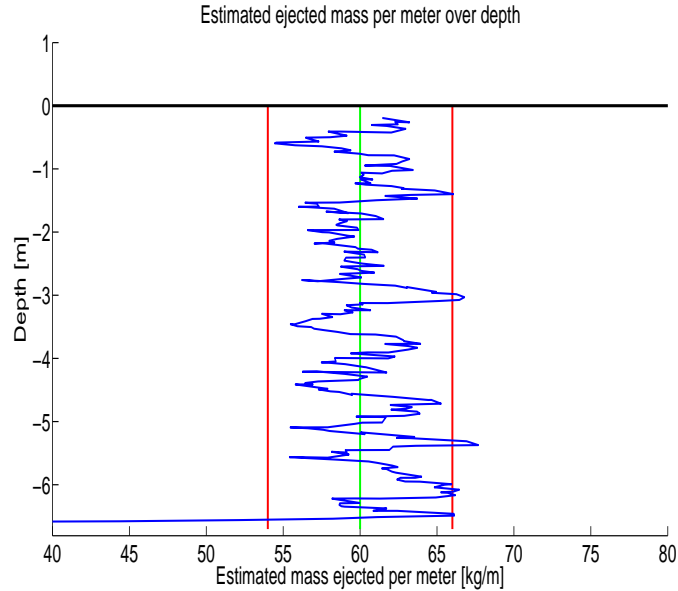
Figure 6.4: *Simulation results of an automatically controlled ground stabilization. Ejected mass per meter versus depth of hose outlet.*

Response to set-point changes   Some ground stabilization-projects require the reference value to change at some point during the process. This puts demands on the controller to be able to track set-point changes relatively fast. A simulation, using the same simulation conditions as above, with a set-point change, was conducted and the result can be studied in figures 6.5 and 6.6. At time $t = 70$ s the reference is changed from 60 kg/m to 57 kg/m.

Figure 6.5: *Simulation results of an automatically controlled ground stabilization with a set-point change at time $t = 70$ s.*

As can be observed in the figures, the controller tracks the set-point change relatively fast although the fluctuations are sometimes larger than the set point change. In the simulation, the same control parameters were used as in the previous simulation, see Table C.1, Appendix C. In Figure 6.6 a plot is presented showing the estimated ejected mass per meter versus depth of hose outlet.
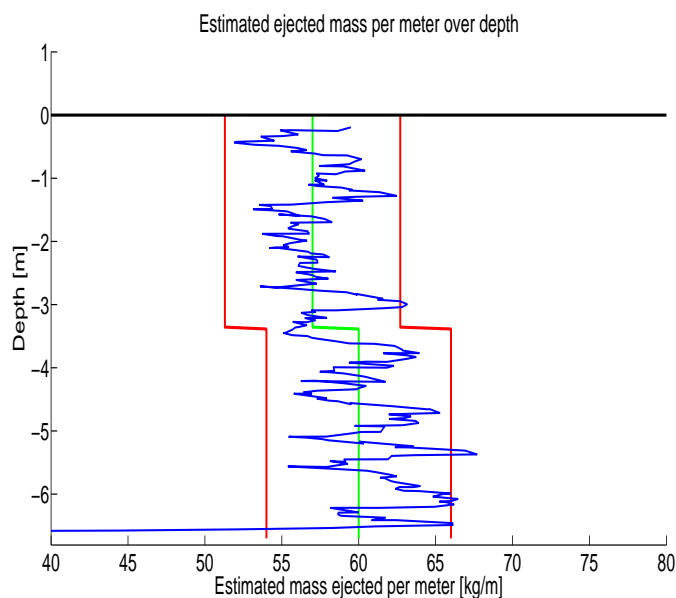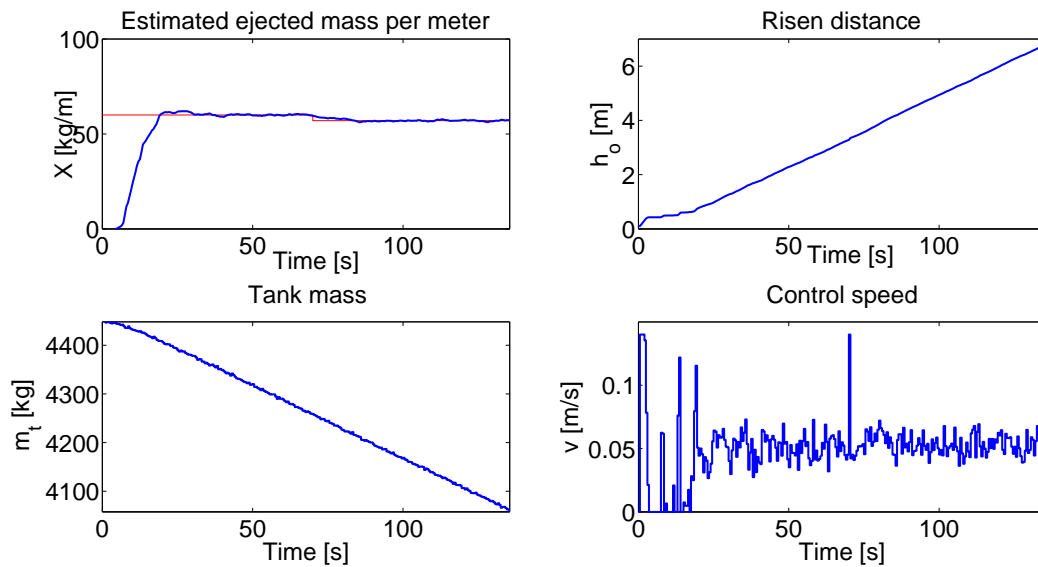

Figure 6.6: *Simulation result of an automatically controlled ground stabilization with a set-point change at time $t = 70$ s. Estimated ejected mass per meter versus depth.*

Decreasing α   In the previous simulations, large disturbances can be observed. By lowering the cut-off frequency(decreasing α) of the first order low pass filter used to filter $\hat{X}$, it is possible to achieve higher performance by tuning the PID-controller again. A simulation with parameters according to Table C.2 in Appendix C was conducted. Results can be observed in figures 6.7 and 6.8.

Figure 6.7: *Simulation result of an automatically controlled ground stabilization.*
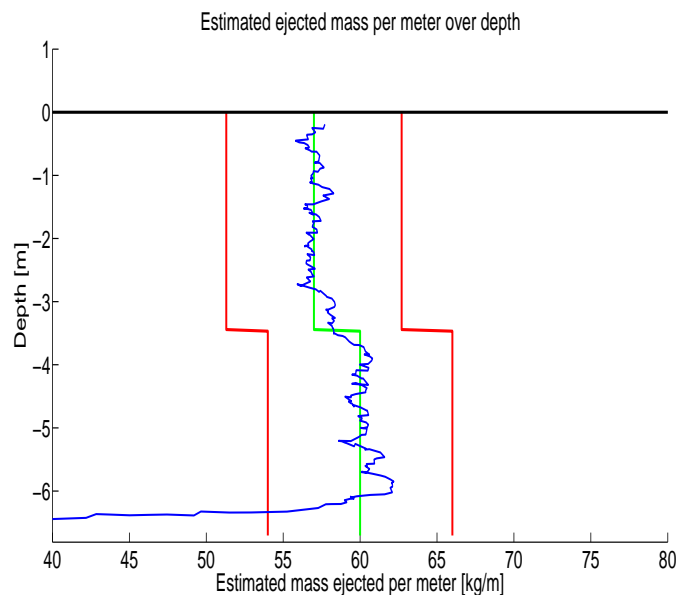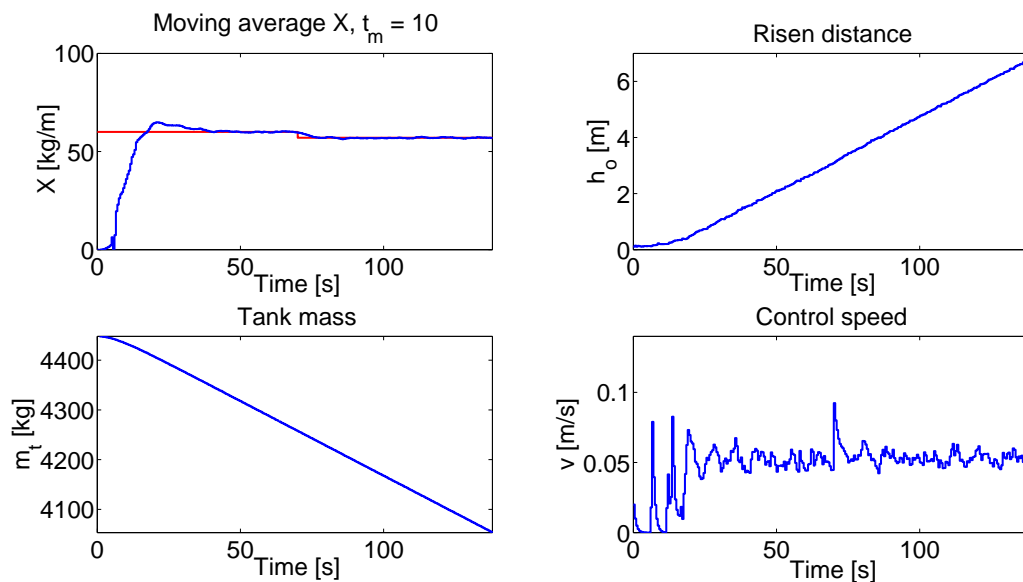

Figure 6.8: *Simulation result of an automatically controlled ground stabilization. Estimated ejected mass per meter versus depth.*

As can be seen in figures 6.7 and 6.8 the set-point is tracked with more accuracy and the response is still relatively fast. It is also easy to observe the superior noise rejection with the smaller filter constant which is now lowered from $\alpha = 0.1$ to $\alpha = 0.02$.

PID$_f$-control An important thing to notice when studying Figure 6.7 in the previous simulation is that the control signal activity has increased substantially. To suppress the control signal activity a low pass filter, with filter constant α_u, is applied on the control signal and again the controller is tuned. To not increase the phase delay too much, the filter constant for the controller is chosen large compared to the output filter.

Figure 6.9: *Simulation results of an automatically controlled ground stabilization with filter on the control signal.*

As shown by the plots in figure 6.9 and 6.10 the control signal activity is lowered while the reference tracking performance is not changed noticeably. Parameters used in this simulation can be found in Table C.3 in Appendix C.
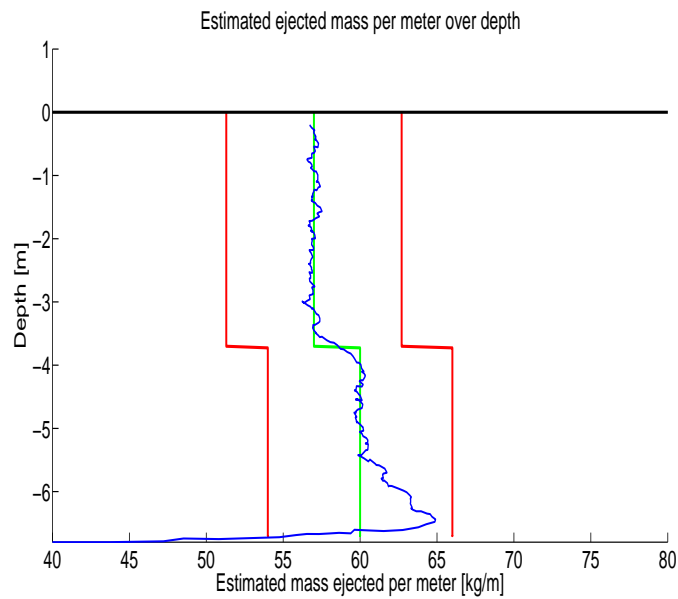
Figure 6.10: *Simulation result of an automatically controlled ground stabilization with filter on the control signal. Estimated ejected mass per meter versus depth.*

Control with FIR-filter on the process output   When controlling with a FIR low pass filter on the process output, the constant delay introduces problems for the controller. The high filter order needed to remove disturbances yields a delay which causes the control action to be applied too late. This can be shown by studying the simulation results in Figure 6.11 where four FIR low pass filters with increasing filter order were evaluated for control purpose.
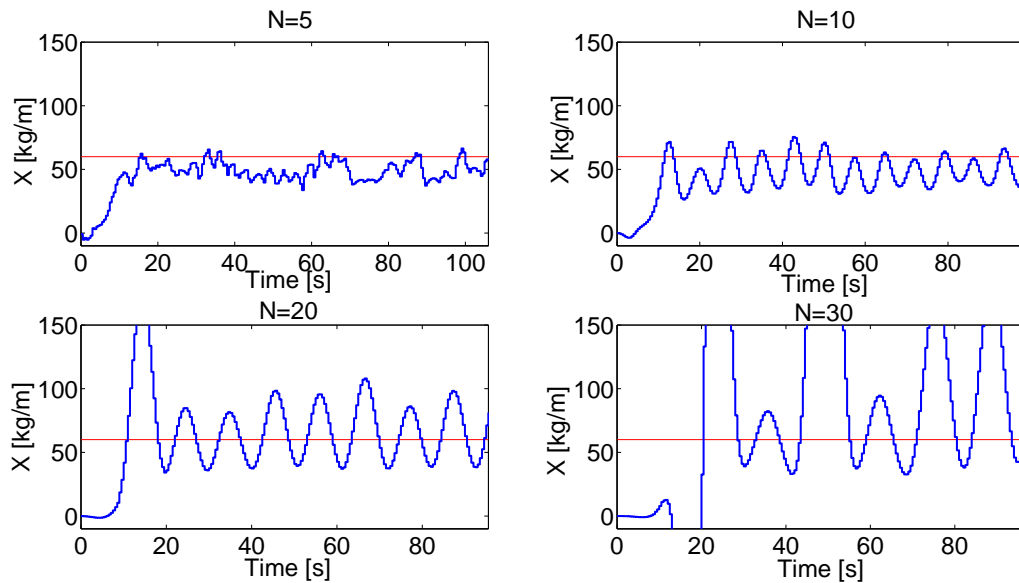
Figure 6.11: *Estimated ejected mass per meter over time for four different FIR low pass filters of order N.*

In the figure, N is the filter order and as shown by the plots in the figure, the set-point tracking performance decreases with higher filter order. At the same time, with low filter order, the disturbance rejection is not sufficient.

6.2.3 Discrete Step D-control

The PID_f-controller is to be compared with a discrete step controller similar to the one currently used by the function responsible for automatic control of the process. The discrete step controller checks if the magnitude of the current error exceeds a certain tolerance level. If this is the case, the algorithm changes the rise speed in discrete steps with a magnitude dependent on in which range the error difference is. The value that the control signal can hold is limited to a few discrete steps. This type of controller was simulated in MATLAB/Simulink were the PID_f-controller was replaced with a function block containing Algorithm 1 which has the error, e, the previous error, e_{prev}, and the previous control signal, u_{prev} as input and outputs the control signal, u.

Algorithm 1 Discrete step controller

    if $|e| < l_{tolerance}$ **then**
        $u = u_{prev}$
    else
        $e_{diff} = e - e_{prev}$
        if $l_1 \leq |e_{diff}| < l_2$ **then**
            $u = v_{norm} + sgn(e_{diff}) * k_1$
        end if
        if $l_2 \leq |e_{diff}| < l_3$ **then**
            $u = v_{norm} + sgn(e_{diff}) * k_2$
        end if
        if $l_3 \leq |e_{diff}| < l_4$ **then**
            $u = v_{norm} + sgn(e_{diff}) * k_3$
        end if
        if $l_4 \leq |e_{diff}| < l_5$ **then**
            $u = v_{norm} + sgn(e_{diff}) * k_4$
        end if
        if $l_5 \leq |e_{diff}|$ **then**
            $u = v_{norm} + sgn(e_{diff}) * k_5$
        end if
    end if

In the algorithm, v_{norm} is the normal speed which is increased or decreased when the error difference is in a certain range. The tolerance level is denoted by $l_{tolerance}$. The limits for the ranges are denoted by l_i where

$$l_5 > l_4 > l_3 > l_2 > l_1 > l_{tolerance}$$

and the constant values, which the normal speed is decreased or increased with, are denoted by k_n and here

$$k_5 > k_4 > k_3 > k_2 > k_1$$

which means that the magnitude of the increase or decrease of the normal speed is larger for larger error differences. Simulating using this type of controller together with the state space model yields the results displayed in figures 6.12 and 6.13.
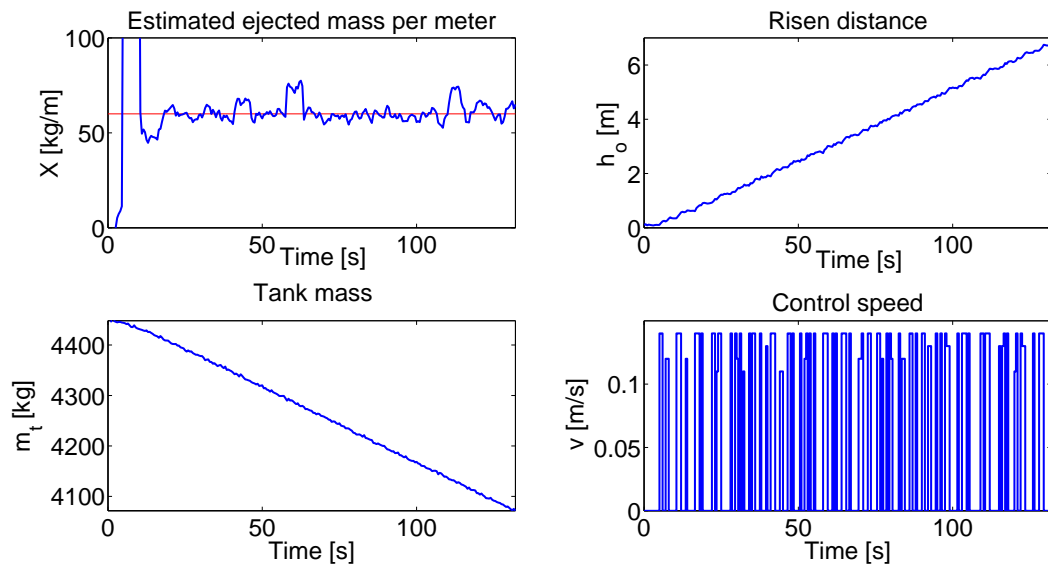
Figure 6.12: *Simulation results of an automatically controlled ground stabilization with a discrete step controller.*

In this simulation, a moving average filter was used both for estimating the ejected mass per meter and for disturbance rejection on the quantity. This is to resemble the configuration used, for control and filtering, currently in the system. Both moving average filters uses 10 samples for calculation. The pressure difference is set to 2.5 bar and band-limited white noise is added on the tank mass and hose outlet position.
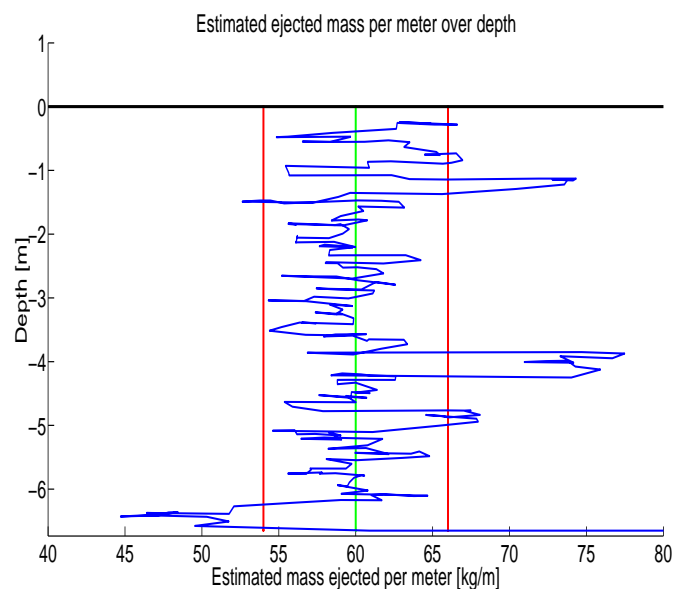
Figure 6.13: *Simulation result of an automatically controlled ground stabilization with a discrete step controller. Estimated ejected mass per meter versus depth.*

The control algorithm manages to keep the estimate around the reference value with quite substantial variations and the process output is sometimes outside the tolerance levels. The performance is higher when using the PID_f-controller. The PID_f-controller is also superior when it comes control signal activity. From Figure 6.12 the discrete jumps of the control signal, which never settles, can be observed. It can be concluded from these simulations that changing the control configuration to PID_f-control should be considered.

6.2.4   Total Error and Steady State Detection

In the controller goals it was stated that the magnitude of the total error in steady state should be below 0.5 kg/m. To calculate this, a steady state detection algorithm is needed. The steady state algorithm and total error is calculated according to Algorithm 2.

Algorithm 2 Steady state and total error calculation

---
   for $i := 2$ **to** T_{stop} **do**
     if $|\hat{X}_f(i) - \hat{X}_f(i-1)| < e_{threshold}$ **then**
       $I = i$;
       $break$;
     end if
   end for
   $e_{tot} = |X_{ref} - \frac{m_o(T_{stop}) - m_o(I)}{h_o(T_{stop}) - h_o(I)}|$;

In the algorithm, T_{stop} is the stop time for the simulation and I is the index where steady state was detected. $e_{threshold}$ is the threshold for the difference between the current and the previous value for the filtered estimate of X. When the difference is smaller than the threshold, steady state is considered found. The way this algorithm is constructed, it only works when there is no set-point change. The total error, e_{tot}, is calculated as the difference between the reference value and the cumulative mass ejected divided with the total distance risen from I to T_{stop}. The algorithm is developed with inspiration from (Karlsson 2008).

Controlling the cumulative ejected mass per meter   One of the most important aspects when controlling the process is that the cumulative ejected mass is not too high or too low. One approach to consider is to instead of feeding back the estimated ejected mass per meter, feed back the cumulative ejected mass divided by the risen distance.

$$X_{tot}(t) = \frac{m_o(t)}{h_o(t)}$$

Thus, $X_{tot}(t)$ is the cumulative ejected mass over the risen distance at time t. A simulation with this configuration was conducted and the result can be observed in

Figure 6.14. In the plot, the cumulative ejected mass per meter is plotted instead of the estimated ejected mass per meter.
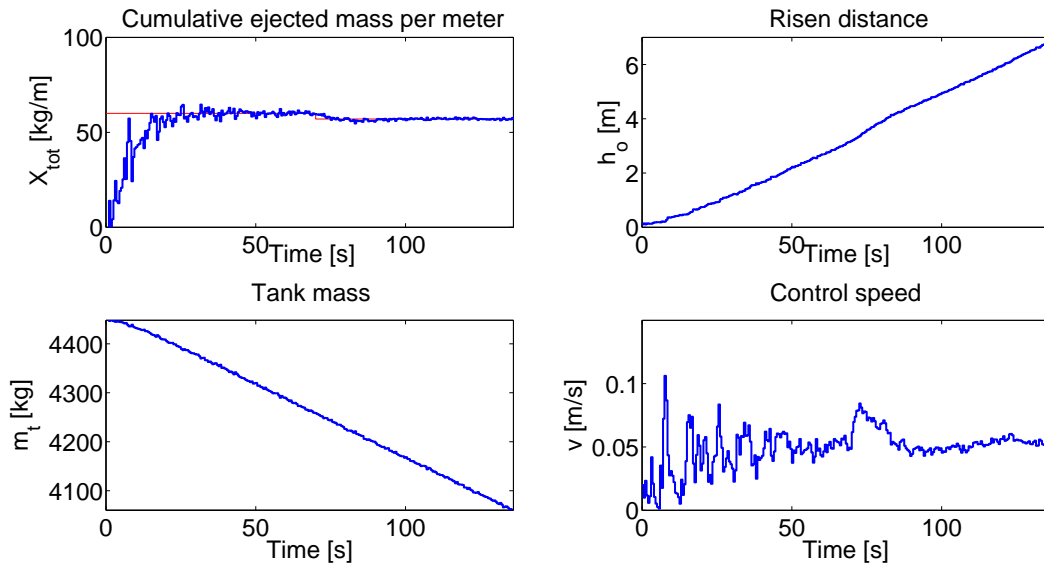
Figure 6.14: *Simulation results of an automatically controlled ground stabilization with feed back of the cumulative ejected mass per meter.*

The result in the figure above looks satisfying and the total ejected mass per meter is tracking the reference well. However, when studying the estimated ejected mass per meter in Figure 6.15 it is obvious that the process output is outside the tolerance levels for a large part of the procedure and not tracking the reference well.
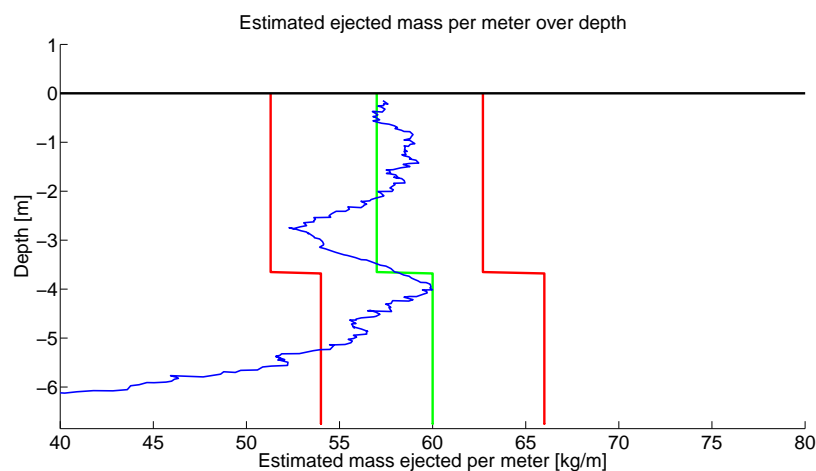
Figure 6.15: *Simulation result of an automatically controlled ground stabilization with feedback of the total ejected mass per meter. Estimated ejected mass per meter over depth.*

It can be concluded from the investigations in this chapter that a suitable way of increasing the control performance for the process is to use a moving average estimation of the ejected mass per meter together with a first order low pass filter to obtain the process output for control purposes. The PID_f-controller proved suitable for tracking the reference and suppressing control signal activity.

7 Implementation

In this chapter, the results of the implementation are presented and compared to the previous filter and control methods used in the process. Results include the implementation of a first order low pass filter and a PID controller. Implementations have been made using a programming language called Cicode and simulated in a SCADA environment developed by AcobiaFLUX.

7.1 SCADA

PLC is one of the most commonly used systems for control in industry. When it is needed to monitor and control several PLC units, a SCADA system may be used to centralize the system. A SCADA system gathers information from the units, sends control actions if needed and displays information in a graphical interface (Bailey and Wright 2003). CitectSCADA includes a programming language called Cicode which is the language used for implementation in this thesis.

7.2 Filter Implementation

A first order low pass filter is implemented as a function in Cicode. The function has access to two arrays, one holding raw values and one holding filtered values. It reads the current index, i, and update the array holding the filtered values according to

$$FilterArray[i] = Alpha * RawArray[i] + (1 - Alpha) * FilterArray[i - 1];$$

Here, *Alpha* is the filter constant, *FilterArray* is the array holding the filtered values and *RawArray* is the array holding the raw values. This function is called after the moving average estimation has been made. The same algorithm is utilized for PID_f-control.

7.3   Controller Implementation

The controller is implemented as a function in Cicode. How the function operates can be studied in Algorithm 3.


Algorithm 3 Calculate control signal

$e_c = \hat{X} - X_{ref}$;
$e_s = e_s + e_c$;
$e_d = e_c - e_p$;
$u_{prel} = v_{norm} + K_p * e_c + K_i * e_s + K_d * e_d$;
if $u_{prel} < u_{min}$ **then**
    $u = u_{min}$;
end if
if $u_{prel} > u_{max}$ **then**
    $u = u_{max}$;
end if
$u = u - (u_{prel} - u) * K_{aw}$;
if $u < u_{min}$ **then**
    $u = u_{min}$;
end if
if $u > u_{max}$ **then**
    $u = u_{max}$;
end if
$setControlSignal(u)$;
$e_p = e_c$;

In the algorithm u_{prel} is the unsaturated control signal and u is the control signal sent to the process. K_p, K_i and K_d are the parameters of the PID-controller and K_{aw} is the anti-windup gain. The current error, e_c, is multiplied with the proportional gain. The total error, e_s, is calculated as the sum of the errors. In the end of the algorithm, the current error is stored as the previous error. The error difference, e_d, is calculated as the difference between the current error and the previous error and multiplied with the derivative gain. When calculating the control signal, an offset, v_{norm}, is added. This is since the control signal should revolve around this normal speed and not zero. The algorithm checks if the preliminary control signal exceeds the maximum limit or fall below the minimum limit and then saturates it. After the anti-windup calculation, this check is performed once again. This is since if K_{aw} is chosen badly, the control signal sent to the process might be higher than the maximum limit or lower than the minimum limit. When PID$_f$ control is used, low pass filtering is performed before sending the control signal.
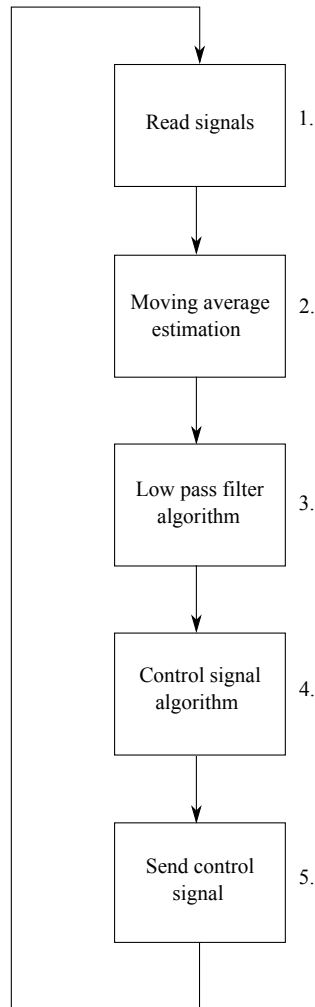
Figure 7.1: *Flow chart of the program containing low pass filtering and control algorithms.*

In Figure 7.1 an overview of the program code used for controlling the process is shown. In the figure, blocks 3 and 4 are the parts implemented during this thesis. The moving average estimation was already implemented. As opposed to the moving average estimations studied in this thesis which is using a time span, a preset length span is used. Benefits of using a length span instead of a time span is that division with zero is avoided.

7.4   SCADA Simulations

The process is modeled as follows in the SCADA-environment. The time rate of the ejected mass is constant with an added random number acting as disturbance. This means that every sample period, an equal amount of mass is being ejected with a small added disturbance. The risen distance is modeled to increase a certain length dependent on the range of the dimensionless integer used to control the

rise speed. If the integer is high, the change of the risen distance will be high. Also here an added random number acts as disturbance. When implementing the algorithms described above and simulating the process in the SCADA environment the process is monitored and plotted as shown in figures 7.2 and 7.3. Parameters used in the implementation can be found in Table C.4 in Appendix C. In the figures, the simulation results of the implemented algorithms and the previous configuration used for control are compared. In figures 7.2a and 7.3a a PID_f controller is used to control the process and a first order low pass filter is used for disturbance rejection on the process output. In figures 7.2b and 7.3b a discrete step controller is used for control and a moving average filter is used to filter the process output. In both cases the span for the moving average estimation of the process output is 1 meter and in the case of the discrete step controller a span of 2 meters is used for moving average filtering of the process output.

(a) PID_f control.   (b) Previous configuration.
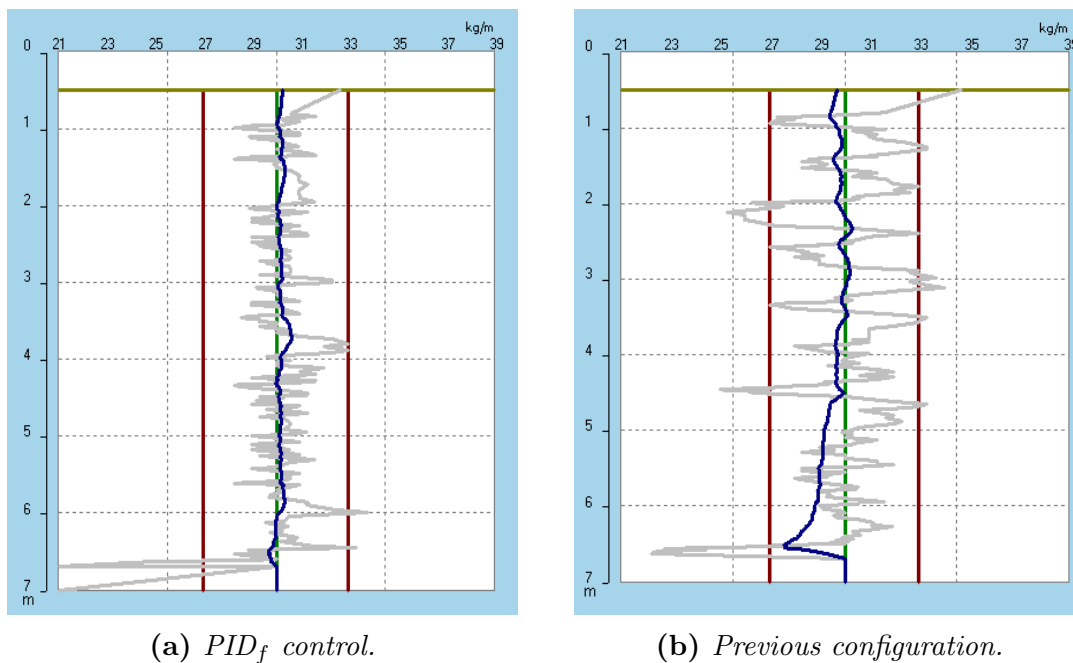
Figure 7.2: *SCADA plots comparing the current filter and control configuration with PID_f control.*

In Figure 7.2 a plot monitoring the process is shown. Here, the reference value for the ejected mass per meter is 30 kg/m. The grey graph represents the unfiltered values for the estimated ejected mass per meter and the blue graph represents the filtered values. The green line represents the reference value and the red lines represent the tolerance levels. Figure 7.3 has a set-point change from 30 kg/m to 29 kg/m at a depth of 5 m.

(a) *PID$_f$ control.*   **(b)** *Previous configuration.*
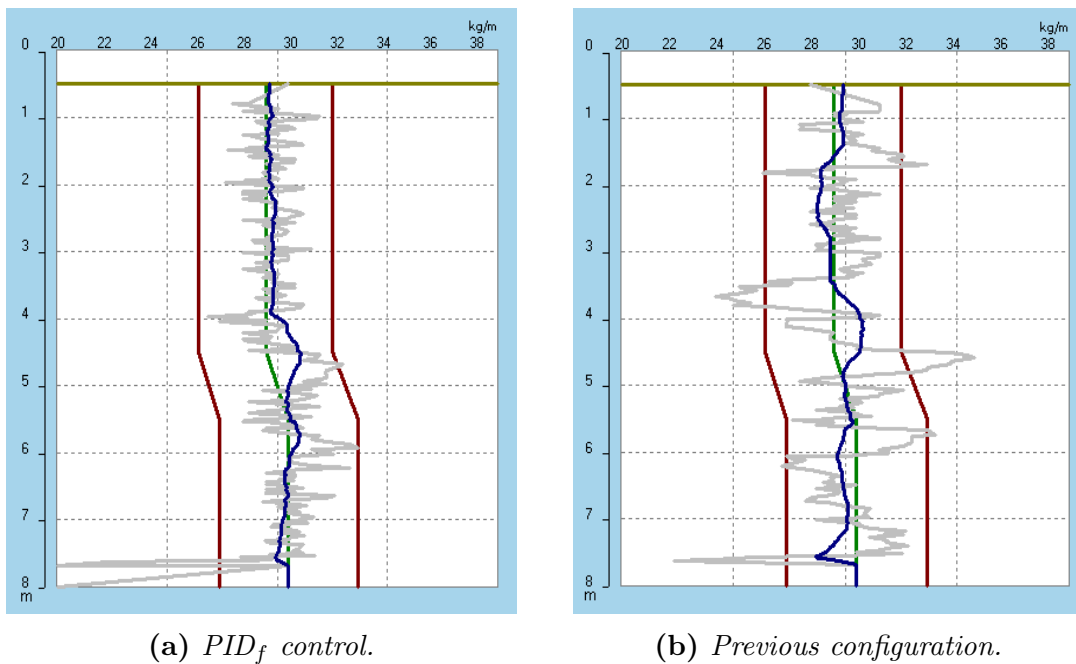
Figure 7.3: *SCADA plots comparing the current filter and control configuration with the new PID$_f$ control.*

When the material between the tip of the tool and the hose outlet is being ejected a straight line is drawn and the amount of mass ejected is assumed to follow the reference value here. This can be observed in the bottom of the plots. From the SCADA-simulations an improvement in both reference tracking and disturbance rejection can be observed.

7.5   Experiments on a Real Machine

A couple of experiments were conducted on a real ground stabilization machine. The same code and the same PID-parameters that was used in the SCADA simulations was implemented in the system. The machine available for experimentation was currently occupied with a project creating very long pillars. First, two pillars using the old configuration was created followed by two using the configuration investigated in this thesis. The result of the experiments can be seen in figures 7.4 and 7.5. Figures 7.4a and 7.4b show the result when using the current old algorithms. Figures 7.5a and 7.5b show the results from an experiment with the configuration investigated in this thesis.

(a) *Experiment 1*   **(b)** *Experiment 2*
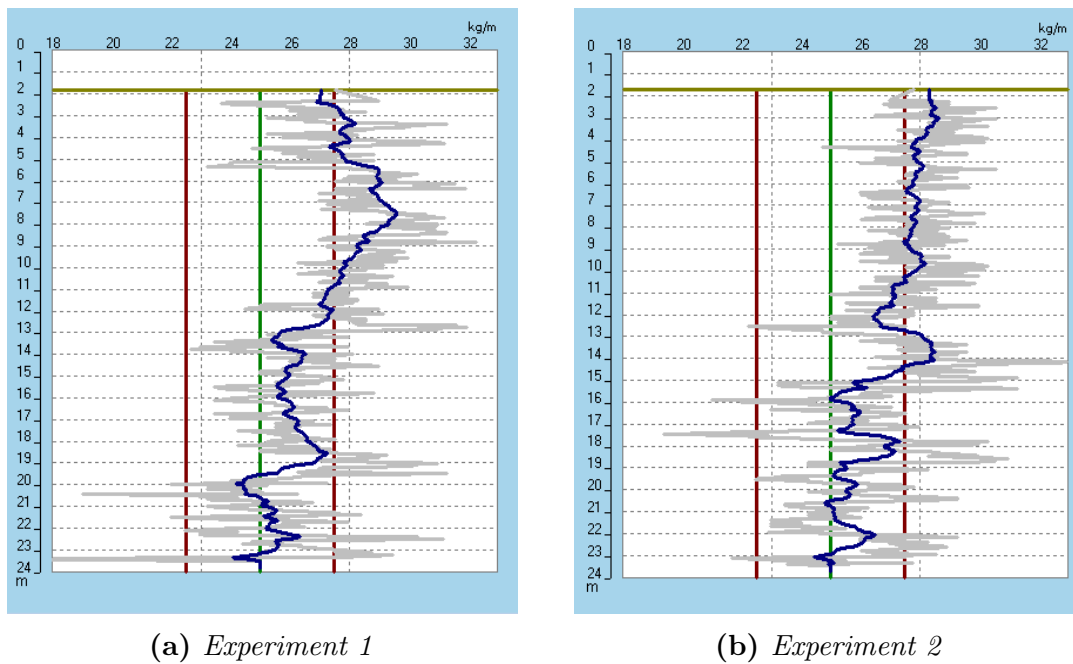
Figure 7.4: *SCADA plots from a real process comparing using the old configuration for control.*

(a) *Experiment 3*   **(b)** *Experiment 4*
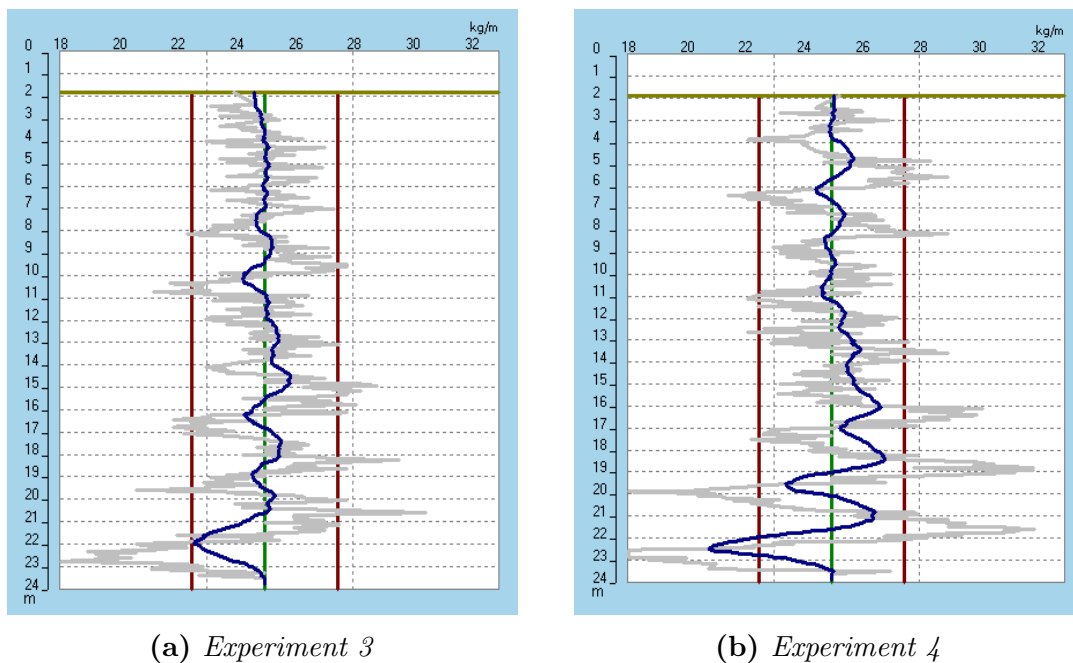
Figure 7.5: *SCADA plots from a real process with PID_f-control.*

In the figures, an improved reference tracking can be observed when using the PID_f-controller although in Figure 7.5b there are some oscillations in the beginning. The estimated ejected mass per meter should not be below the lower tolerance limit for a long time. If that happens, the pillar will not be approved and they will have

to make a new pillar. This can be solved by setting the rise speed to zero when the lower tolerance limit is reached.

The company explained that the current algorithm worked in the beginning for the long pillars but often drifted away from the reference when the tool came closer to the surface. A possible cause of this might be the decreased hardness in the ground when the hose outlet is closer to the surface. As can be seen in the figure, the PID$_f$-controller seems to be able to compensate for this. They also explained that the performance was greatly affected by the quality of the ground.

8 Discussion and Conclusion

In this chapter the findings in the thesis are discussed and concluded. First, general aspects of the thesis are discussed followed by more narrow discussions concerning the mathematical model, filter design, control design and implementation. In the end of the chapter, the thesis is concluded in a short and concise way.

8.1 Discussion

In this thesis, different ways of estimating the ejected mass per meter in a ground stabilization process have been investigated. This has been followed by investigations on ways of removing disturbances from this estimate. The purpose of estimating and filtering this quantity is to automatically control the process using a set-point value for the ejected mass per meter. A mathematical model of the process was derived in order to perform simulations and study the behavior during different estimation, filter and control configurations. Although the model is based on a number of assumptions and approximations, it captures the main characteristics of the process. The purpose of the model was to be able to simulate the effect of filters and controllers for which the model is considered sufficient. Since most of the parameters used in the process are rough approximations, the quantities used in simulations may not coincide with the ones of the real process. The fact that simulations had to use a pressure difference of 2.5 bar to have the ejected mass per meter revolve around the nominal value, instead of 5 bar which was the assumed value in the model, shows that some parameters might be approximated incorrectly. Easy access to the real process would have provided the opportunity to use system identification tools to obtain a model of the system which might have been more accurate. This is provided that the rise speed is measured and logged to the database.

Simulation experiments showed that calculation of the quantity using flow and the rise speed was not suitable due to division by zero at some points. Instead it was more suitable to estimate the quantity with ejected mass and hose outlet position over a certain time using a moving average filter. The use of FIR and FIR differentiator filters for low pass filtering and estimation was researched but shown to be inferior to the first order low pass filter. Most probably because the noise sensitivity of the differentiation. The high filter order needed for the FIR filter to yield a desired disturbance rejection gave rise to a time delay which caused the system to be oscillatory when used for control. The first order low pass filters low phase delay for low frequencies was proven valuable for the purpose of control. Thus the moving average estimation of the ejected mass per meter was combined with a first order low pass filter. Instead of low pass filtering the measured signals, the

estimate was filtered in order to avoid asymptotic offsets in the signals.

The controlled output of the complete process being an estimate involving two outputs of the mathematical model introduced a non-linearity which made linear control design methods not suitable. Instead PID and PID_f control with anti-windup was investigated. The design procedure consisted of tuning the parameters until a desired response of the closed loop system was attained. The controller was compared to a discrete step controller. The discrete step controller was designed to resemble the algorithms currently used in the system. In that way, it was possible to compare the two. The PID_f proved to track the reference faster and reject disturbances more while having less control signal activity.

When implementing and simulating the filters and controller in the SCADA environment, it was difficult to get a satisfying result when applying the proportional gain on the filtered error, instead the unfiltered signal had to be used. Also here, the time delay might be the cause. The filtered signal worked better for the integral and derivative part. The variable holding the rise speed in the program is a unit less integer in the range of approximately 0 - 3900. This of course was a factor when implementing the controller which could not use the same parameters as was designed. Although the ratios between the P, I and D-gains were approximately the same. The accuracy of the model used in the SCADA-environment may be questioned since it includes very little dynamics of the process. For future work, a discretized mathematical model is recommended to be included, in the SCADA-environment, to model the process. More thorough estimation of the parameters of the process is also suggested.

Experiments on a real machine show improved performance compared to the old configurations. However, the experiment was only performed on one machine, using one reference value and one pillar length. Further experiments using different settings are probably wise in order to see that the implementation works all the time. Different parameters for the controller and different normal speeds might be suitable for different pillar types. Perhaps these are settings that should be tuned from the user interface. The oscillations in the beginning of the experiment is most probably caused by variations in the ground. These variations are probably the biggest contributing factor to the process noise. This low frequency process noise might be dominating measurement disturbances. It is intuitive to think that the process is disturbed when the drilling tool reaches harder or softer ground. An extreme case is when the drilling tools hits a rock.

8.2   Conclusion

The objectives of the thesis was to construct a mathematical model of the process, design a filter for disturbance rejection and design a controller for automatic control of the process. These objectives have been fulfilled and there are a couple of things that can be concluded from the thesis:

- The mathematical model was useful for evaluating filters and control configurations, although most parameters of the model are rough estimates and not true.

- A moving average filter showed to be a useful way of estimating the quantity, *ejected mass per meter*.

- When filtering the output signal for control of the process, the phase delay must be kept low in order to achieve high performance.

- The use of PID and PID_f controllers proved to be suitable for control of the process and simulations showed improvements in the performance compared to the current system. Simulation results showed that the estimated ejected mass per meter is kept within the tolerance levels and the magnitude of the total error was kept below 0.5 kg/m in steady state.

- Easy access to the real process would have provided the opportunity to validate the mathematical model, filter and controller and furthermore construct a model using system identification tools which is suggested for future work.

- Experiments on a real machine shows that the PID_f-controller probably is an improvement compared to the algorithms used before.

- Process disturbances is probably the dominating noise factor. Most of the disturbances are probably caused by variations in the ground.

Bibliography

Bailey, D. and Wright, E. (2003). *Practical SCADA for Industry*. Elsevier Ltd.

Bennett, S. (1993). *A History of Control Engineering 1930-1955*. Peter Peregrinus, Ltd. London.

Dmixab (2014-02-06). Projekt i sverige. *http://http://www.dmixab.se/Referenssverige.html*.

Dmixab (2014-03-12). [picture of a ground stabilization machine]. *http://http://www.dmixab.se/Bilder1.html*.

Egardt, B. (2013). Model predictive control lecture notes. Göteborg.

Everitt, B.S. (2002). *The Cambridge Dictionary of Statistics*. Cambridge University Press.

Karlsson, J. (2008). Automatic control of a roller mill using simulations and experiments on a real machine. Master's thesis. Chalmers University of Technology. Göteborg.

Lennartson, B. (2000). *Reglerteknikens grunder*. fourth edn. Studentlitteratur. Lund.

Ljung, L. and Glad, T. (1994). *Modeling of Dynamic Systems*. Prentice Hall, Inc. Upper Saddle River.

Mulgrew, B., Grant, P. and Thompson, J. (2003). *Digital Signal Processing: Concepts and Applications*. Palgrave Macmillan.

Sheikh, Z. Ullah, Eghbali, A. and Johansson, H. (2011). Linear-phase fir digital differentiator order estimation. Linköping, Sweden.

Tarbouriech, S., Garcia, G., da Silva Jr, J.M. Gomes and Queinnec, I. (2011). *Stability and Stabilization of Linear Systems with Saturating Actuators*. Springer.

Visioli, A. (2014). *Practical PID-Control*. Springer. London.

Appendix A

Ramp Offset Derivation

In this appendix a derivation of the asymptotic offset obtained when filtering a ramp signal with a first order low pass filter is presented. The derivation uses the discrete version of the final value theorem as starting point.

$$
\begin{aligned}
\lim_{i \to \infty} (y_f(i) - y(i)) &= \lim_{z \to 1} (Y_f(z) - Y(z))(z - 1) \\
&= \lim_{z \to 1} Y(z)(F_{LP}(z) - 1)(z - 1) \\
&= \lim_{z \to 1} \frac{z}{(z - 1)^2} (\frac{\alpha z}{z - 1 + \alpha} - 1)(z - 1) \\
&= \lim_{z \to 1} \frac{z}{(z - 1)^2} (\frac{\alpha z}{z - 1 + \alpha} - \frac{z - 1 + \alpha}{z - 1 + \alpha})(z - 1) \\
&= \lim_{z \to 1} \frac{z}{(z - 1)^2} (\frac{\alpha z - z - \alpha + 1}{z - 1 + \alpha})(z - 1) \\
&= \lim_{z \to 1} \frac{z}{(z - 1)} (\frac{\alpha z - z - \alpha + 1}{z - 1 + \alpha}) \\
&= \lim_{z \to 1} \frac{z(z - 1)(\alpha - 1)}{(z - 1)(z - 1 + \alpha)} \\
&= \lim_{z \to 1} \frac{z(\alpha - 1)}{(z + (\alpha - 1)} \to 1 - \frac{1}{\alpha}
\end{aligned}
$$

Appendix B

Simulation Set Up

In this appendix, the set up for simulation experiments are explained. Simulations were performed in MATLAB and Simulink. The main program runs in MATLAB, in the program there are a couple of steps:

- *Input data* - First, one chooses which input data should be used in the simulation.

- *Parameters* - The filter constants/coefficients, moving average spans, $\text{PID}(_f)$-paramters, anti-windup gain are declared.

- *Run simulation* - Run the Simulink model using the input data and parameters. The simulation stops when the hose outlet has reached a desired position.

- *Plot data* - Return to MATLAB-program and plot results.

Available Simulink models are

- Flow estimation

- First order low pass filtering

- FIR and FIR-differentiator filtering

- $\text{PID}(_f)$ with anti-windup control

- Discrete step control

- Control of cumulative ejected mass per meter

where all of them uses the state space model.

Appendix C

Simulation Parameters

In this appendix, parameters used in simulations are presented. In tables C.1, C.2 and C.3, parameters used in Simulink simulations are found. In Table C.4 parameters implemented in the SCADA environment are found.

Parameter	Notation	Value
Proportional gain	K_p	0.001
Integral gain	K_i	0.0002
Derivative gain	K_d	0.001
Anti wind-up gain	K_{aw}	0.1
Filter constant	α	0.1
Moving average span	t_m	10

Table C.1: *Simulation parameters for the first control simulation using PID control.*

Parameter	Notation	Value
Proportional gain	K_p	0.01
Integral gain	K_i	0.002
Derivative gain	K_d	0.04
Anti wind-up gain	K_{aw}	0.1
Filter constant	α	0.02
Moving average span	t_m	10

Table C.2: *Simulation parameters for the seconds control simulation using a lower value on the filter constant.*

Parameter	Notation	Value
Proportional gain	K_p	0.01
Integral gain	K_i	0.001
Derivative gain	K_d	0.04
Anti wind-up gain	K_{aw}	0.1
Filter constant	α	0.02
Filter constant	α_u	0.5
Moving average span	t_m	10

Table C.3: *Simulation parameters used for the third control simulation using PID$_f$ control.*

Parameter	Notation	Value
Proportional gain	K_p	200
Integral gain	K_i	5
Derivative gain	K_d	20
Anti wind-up gain	K_{aw}	0.1
Filter constant	α	0.04
Filter constant	α_u	0.5
Moving average span	l_m	1 m

Table C.4: *Parameters implemented and simulated in the SCADA environment.*